THE COMPANY OF
Biologists

RESEARCH ARTICLE

Oncogenic K-Ras suppresses IP$_3$-dependent Ca^{2+} release through remodelling of the isoform composition of IP$_3$Rs and ER luminal Ca^{2+} levels in colorectal cancer cell lines

Cristina Pierro, Simon J. Cook, Thomas C. F. Foets, Martin D. Bootman* and H. Llewelyn Roderick[‡]

ABSTRACT

The GTPase Ras is a molecular switch engaged downstream of G-protein-coupled receptors and receptor tyrosine kinases that controls multiple cell-fate-determining signalling pathways. Ras signalling is frequently deregulated in cancer, underlying associated changes in cell phenotype. Although Ca^{2+} signalling pathways control some overlapping functions with Ras, and altered Ca^{2+} signalling pathways are emerging as important players in oncogenic transformation, how Ca^{2+} signalling is remodelled during transformation and whether it has a causal role remains unclear. We have investigated Ca^{2+} signalling in two human colorectal cancer cell lines and their isogenic derivatives in which the allele encoding oncogenic K-Ras (G13D) was deleted by homologous recombination. We show that agonist-induced Ca^{2+} release from the endoplasmic reticulum (ER) intracellular Ca^{2+} stores is enhanced by loss of K-Ras^{G13D} through an increase in the Ca^{2+} content of the ER store and a modification of the abundance of inositol 1,4,5-trisphosphate (IP$_3$) receptor (IP3R) subtypes. Consistently, uptake of Ca^{2+} into mitochondria and sensitivity to apoptosis was enhanced as a result of K-Ras^{G13D} loss. These results suggest that suppression of Ca^{2+} signalling is a common response to naturally occurring levels of K-Ras^{G13D}, and that this contributes to a survival advantage during oncogenic transformation.

KEY WORDS: K-Ras, Cancer, Inositol 1,4,5-trisphosphate, IP$_3$, Ca^{2+}, Mitochondria

INTRODUCTION

Ras proteins serve as molecular switches downstream of receptor tyrosine kinases and upstream of the Raf protein kinases (Cully and Downward, 2008; Downward, 2003a; Downward, 2003b; Schulze et al., 2004). This pathway is frequently de-regulated in cancer due to mutation in receptor tyrosine kinases (RTKs) (e.g. EGFR), Ras itself (~20% of all human cancers) and B-Raf (Downward, 2003b). These mutations elicit significant consequences for cell fate owing to their position as upstream regulators of multiple pathways involved in the regulation of cell cycle, metabolism and cell death – hallmarks of the transformed phenotype (Hanahan and Weinberg, 2000; Hanahan and Weinberg, 2011). This central role of Ras and the downstream pathways it engages have been targeted by the pharmaceutical industry in the development of cancer therapeutics. Indeed, drugs targeting the B-Raf–Mek–Erk pathway have now been approved in the clinic (Belden and Flaherty, 2012; Little et al., 2013).

As Ras lies upstream of multiple cellular pathways, redundancy in function between these signal transduction cascades allows transformed cells to overcome drug targeting and develop resistance (Little et al., 2013). Many of these downstream pathways are also dysregulated in cancer (Wu et al., 2013). Understanding the nature of interactions between Ras and other major cellular signalling pathways is therefore essential for development of effective strategies for suppression of Ras-driven cancer (Wu et al., 2013). A major, but as yet undefined, signalling interaction in oncogenic transformation is that between Ras and Ca^{2+}.

Ca^{2+} is a pleiotropic signalling messenger that, like Ras, plays key roles in life and death choices, including the decision to proliferate or die by apoptosis (Berridge et al., 2003) (Berridge et al., 1998). Oscillations in cytoplasmic Ca^{2+} are necessary to sustain the cell cycle, via calmodulin (CaM) (Cullen and Lockyer, 2002; Kahl and Means, 2003), whereas Ca^{2+} overload by the mitochondria is an initiator of the intrinsic apoptotic cascade (Rizzuto et al., 2003). Not surprisingly therefore, deregulation of Ca^{2+} homeostasis has been reported in diseases associated with overt or diminished proliferation and increased or insufficient cell death. Cancer cells are characterized in part by uncontrolled proliferation and apoptosis evasion (Hanahan and Weinberg, 2000; Hanahan and Weinberg, 2011); these characteristics have been proposed to be supported by a remodelling of their Ca^{2+} signalling toolkit (Roderick and Cook, 2008). Indeed, alterations in the expression of a number of Ca^{2+}-handling proteins have been reported in various tumours (Monteith et al., 2007), but attempts to formulate general principles of Ca^{2+} signalling alterations in cancer have thus far failed. Little consistency in the alterations in Ca^{2+} protein expression is found among different tumours and between studies. Moreover, few studies have clarified whether altered Ca^{2+} signalling contributes to the cancer phenotype or is a consequence.

Nowhere is this more apparent than in studies linking Ras to Ca^{2+} signalling, which go back over 25 years and reveal a complex interplay between these pathways. For example, Ras was shown to enhance agonist-regulated inositol 1,4,5-trisphosphate (IP$_3$) production (Hashii et al., 1993; Lang et al., 1991; Wakelam et al., 1986), a result that might be owing to the ability of Ras protein to bind phospholipase C (PLC) ε (Bunney et al., 2006;

Bunney and Katan, 2006). Conversely, Ca^{2+} signalling can activate certain Ras guanine-nucleotide-exchange factors (GEFs) or Ras GTPase-activating proteins (GAPs) to promote or inhibit activation of Ras and Ras-dependent signalling (Cook and Lockyer, 2006; Roderick and Cook, 2008). The normal interplay between these events is complex and is made all the more so in cells expressing mutant oncogenic variants of Ras such as those harbouring missense substitutions at Gly12, Gly13 or Gln61 (Barbacid, 1987), which prevent the hydrolysis of GTP by GAPs, resulting in Ras being permanently active (Bollag and McCormick, 1991). These de-regulated Ras oncoproteins activate several effector pathways and contribute to virtually all of the hallmarks of the cancer cell (Hanahan and Weinberg, 2000; Hanahan and Weinberg, 2011), including promoting cell proliferation and survival. This pleiotropy of Ras undoubtedly contributes to some of the striking cell- and tissue-specific differences in the regulation of Ca^{2+} signalling seen in studies with oncogenic Ras mutants. In addition, however, it is apparent that mutant Ras proteins can elicit quite different effects depending on their expression level. Most strikingly, conditional overexpression of oncogenic K-Ras elicits cell cycle arrest and senescence in primary mouse embryo fibroblasts whereas conditional expression at endogenous levels causes cell proliferation and oncogenic transformation (Tuveson et al., 2004). Thus, although studies employing conditional overexpression of mutant Ras proteins have merits, it is important to confirm results in cell systems with native expression levels of mutant Ras to avoid artefacts arising from overexpression.

To overcome this issue, we have taken advantage of isogenic cell line pairs in which the *KRAS* allele encoding oncogenic K-Ras has been ablated by homologous recombination (Shirasawa et al., 1993). The parental cancer cell line harbouring the mutant allele can then be directly compared with an isogenic derivative that is identical apart from the lack of oncogenic Ras. This approach has the benefit of comparing the effects of a single copy of mutant *KRAS* rather than using supra-physiological expression. Using this approach, we show that oncogenic K-Ras inhibits Ca^{2+} release from the endoplasmic reticulum (ER), reduces ER Ca^{2+} levels and suppresses Ca^{2+} flux to the mitochondria. These results suggest that suppression of Ca^{2+} signalling is a common response to naturally occurring levels of K-Ras^{G13D} that contributes to a survival advantage during oncogenic transformation.

RESULTS

IP$_3$-induced Ca^{2+} release is increased in cells deleted of K-Ras^{G13D}

Although alterations in expression of a number of proteins involved in Ca^{2+} regulation in various tumour types and tumour-derived cell lines have been described (Monteith et al., 2007), few studies have analysed how Ca^{2+} signalling is altered as a result of transformation. Moreover, the nature and role of the effect of the presence of natively expressed 'driving' oncogenes upon Ca^{2+} homeostasis has not been determined. As such, consensus regarding how Ca^{2+} signalling participates in cellular transformation is lacking (Roderick and Cook, 2008). Contributing to this great variability is the problem in identifying appropriate experimental controls for the cancer cells studied and the issues associated with use of experimental systems in which pleiotropic oncogenes are expressed at supra-physiological levels (Tuveson et al., 2004). In this study, we sought to analyse the effects of a single oncogenic allele at physiological expression levels. To this end, we compared

the HCT116 colorectal cancer cell line (K-Ras$^{G13D/WT}$) with its isogenic derivative HKH2 (K-Ras$^{-/WT}$) in which the mutated Ras allele has been deleted by homologous recombination. In contrast to HCT116 cells, HKH2 cells do not grow in soft agar and do not form tumours in nude mice (Shirasawa et al., 1993). We employed these cell lines to evaluate whether the presence of the endogenous oncogenic K-Ras^{G13D} allele modified the generation of Ca^{2+} signals. As shown in Fig. 1, as a consequence of loss of K-Ras^{G13D} in HKH2 cells, Ca^{2+} signals induced following stimulation of purinergic receptors with ATP were enhanced when compared to HCT116 cells (Fig. 1Ai). This difference was evident in the percentage of responding cells (Fig. 1Aii), in the amplitude (Fig. 1Aiii) and in the integral (area under the curve; AUC) of the Ca^{2+} transients (Fig. 1Aiv).

To isolate the contribution of Ca^{2+} influx to the agonist-induced Ca^{2+} transient, experiments were performed in the absence of extracellular Ca^{2+}. As observed in Ca^{2+}-containing buffer, the AUC and responsiveness to agonist (applied at a concentration where the greatest differences in agonist responses were observed in Ca^{2+}-containing buffer) remained greater in HKH2 than HCT116 cells when Ca^{2+} was omitted from the imaging buffer. These data therefore indicated that K-Ras^{G13D} in HCT116 cells was acting to suppress Ca^{2+} release from the ER (Fig. 1B).

To further probe the interaction between Ras and Ca^{2+} signalling in HCT116, Ras expression was also suppressed by small interfering RNA (siRNA). Using this approach, Ras expression was reduced by 85% when compared to HCT116 cells transfected with control non-targeting siRNA (Fig. 2A). siRNA depletion of Ras in HCT116 cells resulted in a significant increase in ATP-stimulated Ca^{2+} signals in these cells (Fig. 2B). The increase in Ca^{2+} signalling was manifest as an increase in the percentage of responding cells and in the amplitude and AUC of the Ca^{2+} responses (Fig. 2Bii–iv). These data are consistent with that observed in HKH2 cells and support the conclusion that the difference between HCT116 and HKH2 cells is due to K-Ras^{G13D} ablation and not a phenotype developed as a result of HKH2 culture since their initial generation.

To test whether the enhanced Ca^{2+} responses observed as a result of K-Ras^{G13D} deletion in HCT116 cells was a general feature of G-protein-coupled receptor (GPCR) signalling in these cells, we examined histamine-induced Ca^{2+} responses, which proceed through a similar GPCR–G$_q$–PLC–IP$_3$ pathway. In response to this agonist, a greater percentage of HKH2 cells exhibited Ca^{2+} transients, which were of a greater amplitude and AUC than those observed in HCT116 cells (Fig. 3A). These data indicated that the alteration in Ca^{2+} fluxes was not specific to differences in purinergic receptor signalling but was a more general effect, involving signals downstream of GPCR engagement.

To directly address whether an alteration in IP$_3$ signalling contributed to the enhancement of ER Ca^{2+} release in cells lacking K-Ras^{G13D}, Ca^{2+} release was induced with a cell-permeant esterified form of IP$_3$ [myo-inositol 1,4,5-trisphosphate hexakis(butyryloxymethyl); IP$_3$BM], which was perfused over the cells in Ca^{2+}-free imaging buffer during the course of the experiment (Conway et al., 2006; Kasri et al., 2004; Thomas et al., 2000). Using this approach, IP$_3$ receptors (IP$_3$Rs) are directly engaged, bypassing GPCR, G$_q$, PLC and endogenous IP$_3$. As in experiments using ATP and histamine, Ca^{2+} signals induced by IP$_3$BM were also greater in HKH2 cells than in their HCT116 counterparts (Fig. 3B).

Given that K-Ras is frequently mutated in colorectal cancer, we investigated whether Ca^{2+} signalling was also remodelled as a
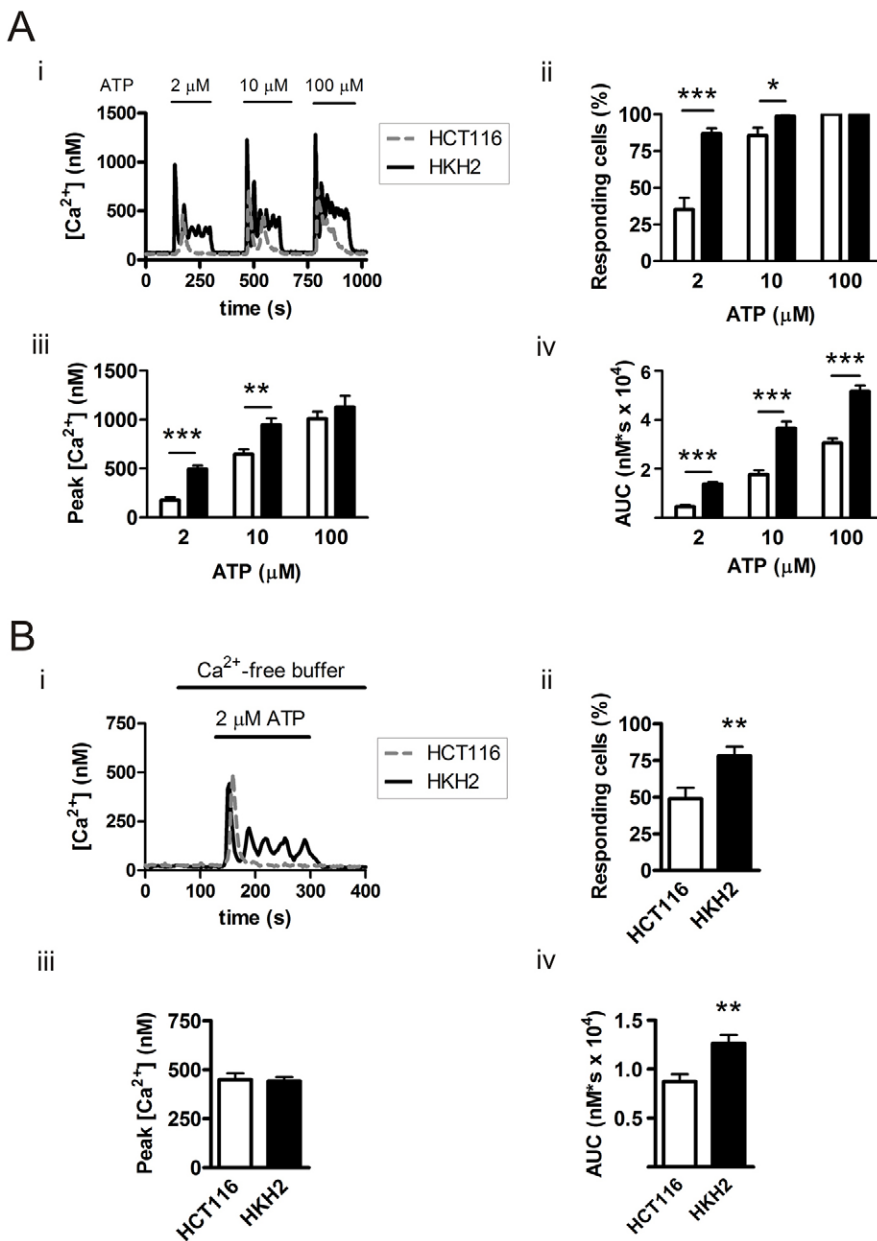
Fig. 1. Agonist (ATP)-induced Ca^{2+} signals are influenced by K-Ras^{G13D} in the HCT116 colorectal cancer cell line. (Ai) Representative ATP-stimulated Ca^{2+} responses of HCT116 and HKH2 cells. Cells were stimulated with ATP at the concentrations indicated and experiments performed in the presence of extracellular Ca^{2+}. (Aii) Percentage of responding cells. (Aiii) Peak amplitude of Ca^{2+} response. (Aiv) Integrated Ca^{2+} response (AUC) of responding cells. Results are means±s.e.m. of data from 4 days of experiments, where three coverslips per cell type were imaged on each day ($n=12$). At least 60 cells per coverslip were analysed. White bars represent HCT116 cells and black bars represent HKH2 cells. (Bi) Representative ATP-stimulated Ca^{2+} responses in HCT116 and HKH2 cells. Cells were stimulated with 2 μM ATP in absence of extracellular Ca^{2+}. (Bii) Percentage of responding cells. (Biii) Peak amplitude of Ca^{2+} response. (Biv) AUC of responding cells. Results are the means±s.e.m. of data from 3 days of experiments, where three coverslips per cell type were imaged on each day ($n=9$). At least 60 cells per coverslip were analysed. *$P<0.05$; **$P<0.01$; ***$P<0.001$ (Student's t-test).

result of loss of K-Ras^{G13D} in a second independent colorectal cancer cell line, DLD-1 (Shirasawa et al., 1993). As performed for HCT116 cells and their isogenic derivatives, experiments were carried out in Ca^{2+}-free imaging buffer to restrict our analysis to Ca^{2+} release from the ER. ATP-induced Ca^{2+} fluxes were greater in the K-Ras^{G13D}-deleted DKO4 cell line (K-Ras$^{-/WT}$) than in their parental isogenic DLD-1 cell line (K-Ras$^{G13D/WT}$) (Fig. 4). This was manifest as an increase in the percentage of responding cells and in the amplitude and AUC of the Ca^{2+} responses (Fig. 4ii–iv). Taken together, these data show that oncogenic K-Ras^{G13D} limits IP$_3$-induced Ca^{2+} release (IICR) in both HCT116 and DLD-1 cells.

ER Ca^{2+} content is increased in cells deleted of K-Ras^{G13D}

Given that the magnitude of Ca^{2+} released from the ER is determined by its state of filling, we hypothesized that the enhanced Ca^{2+} release observed following K-Ras^{G13D} deletion in HKH2 cells was due to an increase in content of the

IP$_3$-releasable ER Ca^{2+} store. To assess ER Ca^{2+} levels, the magnitude of the Ca^{2+} mobilized from the ER by the SERCA pump inhibitor thapsigargin (Tg) was analysed. Through inhibition of SERCA, Tg reveals the non-specific Ca^{2+} leak from the ER causing Ca^{2+} accumulation in the cytosol. As store depletion with Tg also leads to Ca^{2+} influx across the plasma membrane, measurements were performed in Ca^{2+}-free imaging buffer. Application of Tg induced an elevation in intracellular Ca^{2+} in both the HCT116 and HKH2 cell lines (Fig. 5A). The amplitude and AUC of the Tg-induced Ca^{2+} transient was, however, significantly greater in the HKH2 cell line compared to HCT116 cells (Fig. 5Aii,iii).

To complement these data and to accommodate for the indirect nature of using the Tg-induced elevation in cytosolic Ca^{2+} as a measure of ER luminal Ca^{2+} content, the free Ca^{2+} content of the ER was also measured directly using a genetically encoded GFP-based Ca^{2+} indicator targeted to the ER (known as D1ER) (Palmer et al., 2004). This indicator relies upon a Ca^{2+}-dependent
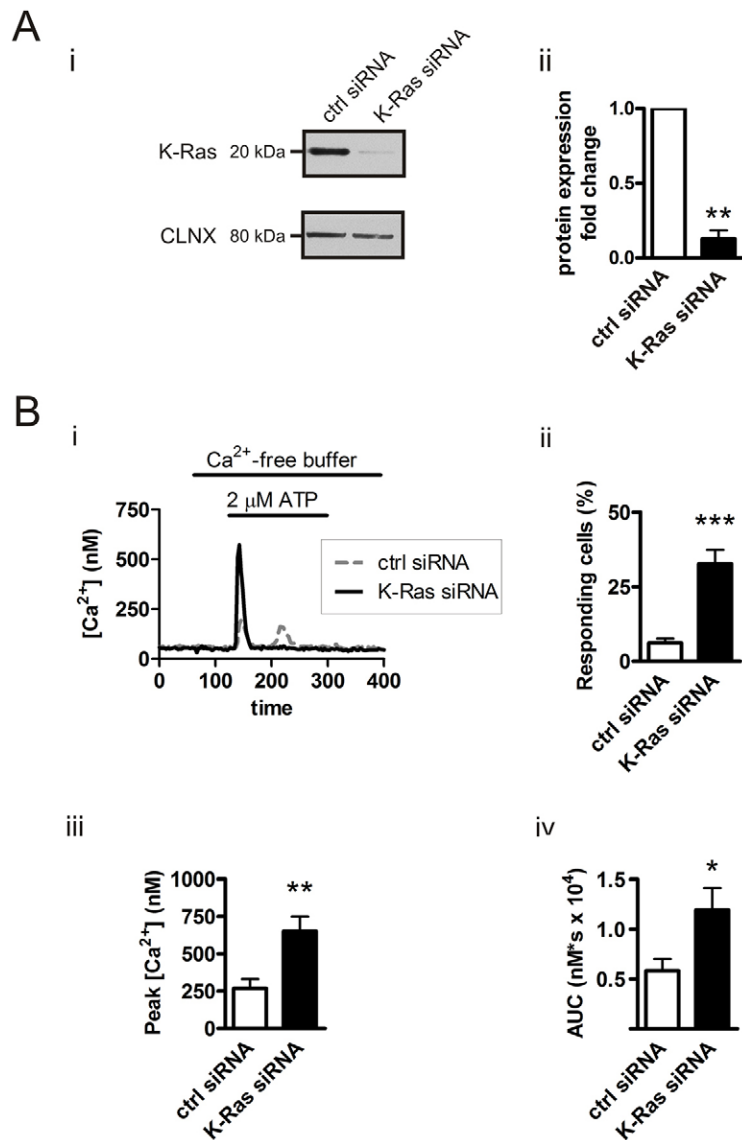
Fig. 2. ATP-stimulated Ca^{2+} responses are enhanced by siRNA depletion of K-Ras in HCT116 cells. (Ai) Representative immunoblot of K-Ras in HCT116 cells transfected with control (ctrl) siRNA or siRNA targeting K-Ras. Calnexin (CLNX) was used as a loading control. (Aii) Quantification of K-Ras knockdown in HCT116 cells ($n=3$). (Bi) Representative Ca^{2+} responses of siRNA-transfected HCT116 cells stimulated with 2 µM ATP in Ca^{2+}-free imaging buffer. (Bii) Percentage of responding cells. (Biii) Peak amplitude of Ca^{2+} response. (Biv) AUC of responding cells. Results are means±s.e.m. of data from 3 days of experiments, where three coverslips per cell type were imaged on each day ($n=9$). At least 60 cells per coverslip were analysed. *$P<0.05$; **$P<0.01$; ***$P<0.001$ (Student's t-test).

change in Förster resonance energy transfer (FRET) between cyan (CFP) and yellow (YFP) derivatives of GFP. D1ER was expressed in a reticular pattern and colocalized with the ER protein calnexin in both cell types, confirming its ER localization (Fig. 5Bi). In resting cells, greater FRET (the YFP:CFP ratio) was observed in the HKH2 cell line than in the HCT116 cell line, indicating higher basal Ca^{2+} in the ER of this cell line (Fig. 5Bii). Application of the Ca^{2+} ionophore ionomycin to fully deplete Ca^{2+} from the ER store resulted in a decline in FRET to a lower plateau, which was equivalent between the two cell types (Fig. 5Bii). The similar Ca^{2+}-free FRET between both cell types indicated that D1ER was behaving equivalently in the two cell types. A ratio of basal FRET to Ca^{2+}-free FRET was therefore used to normalize ER Ca^{2+} levels, which also indicated greater Ca^{2+} levels in the ER of HKH2 than HCT116 cells (Fig. 5Biii).

IP$_3$R isoform expression is remodelled and SERCA2b expression is increased in cells deleted of K-Ras^{G13D}

Having identified that an increase in ER Ca^{2+} contributed to the enhanced Ca^{2+} signalling in K-Ras^{G13D}-deleted cells, an analysis

of proteins involved in ER Ca^{2+} signalling was carried out. In these experiments, as we have employed elsewhere when analysing ER proteins of a high molecular mass (Drawnel et al., 2012; Harzheim et al., 2009), the ER membrane protein calnexin was used as a loading control for normalization of the protein of interest between cell types. Expression of calnexin was found to exhibit a similar expression profile between HCT116 and HKH2 cells as did two other proteins – GAPDH and β-actin – that are routinely used for normalization in immunoblotting (supplementary material Fig. S1). The expression of SERCA2b, which is primarily responsible for ER Ca^{2+} sequestration, was increased in HKH2 cells (Fig. 5C), whereas the expression of calreticulin, the major Ca^{2+} storage protein in non-excitable cells, was not altered between the two cell types (Fig. 5D). Given that SERCA3 upregulation has been reported in cancer (Brouland et al., 2005), its expression was also investigated but found to be unchanged in cells lacking K-Ras^{G13D} (supplementary material Fig. S1). Notably, the expression profile of IP$_3$Rs was significantly different between HKH2 and HCT116 cells. Specifically, IP$_3$R3 (also known as ITPR3) expression was increased and IP$_3$R1 (also known as
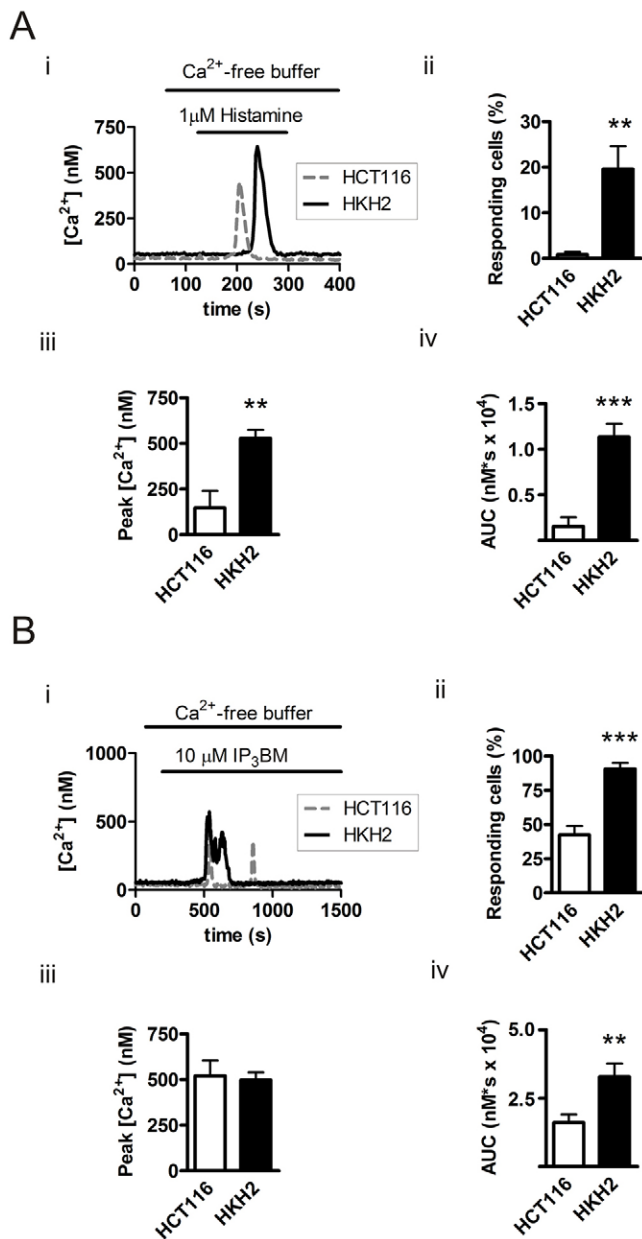
Fig. 4. ATP-stimulated Ca²⁺ responses are controlled by K-Ras^{G13D} in the DLD-1 colorectal cancer cell line. (Ai) Representative Ca²⁺ responses of DLD-1 and DKO4 cells stimulated with 2 μM ATP in Ca²⁺-free imaging buffer. (Aii) Percentage of responding cells. (Aiii) Peak amplitude of Ca²⁺ response. (Aiv) AUC of responding cells. Results are means±s.e.m. of data from 3 days of experiments, where three coverslips per cell type were imaged on each day (n=9). At least 60 cells per coverslip were analysed. *P<0.05; ***P<0.001 (Student's t-test).

Cells deleted of K-Ras^{G13D} exhibit increased mitochondrial Ca²⁺ uptake and sensitivity to apoptosis

Mitochondrial Ca²⁺ uptake is a low-affinity process that occurs in a privileged manner at microdomains of high Ca²⁺ generated by IP₃Rs located at sites where the ER and mitochondria are in close proximity (Csordás et al., 2006; Duchen, 2000; Rizzuto et al., 1998; Rizzuto and Pozzan, 2006). Ca²⁺ flux from ER-localized IP₃Rs to the mitochondria has been shown to play an important role in regulation of cell death and metabolism (Cárdenas et al., 2010; Pinton et al., 2001) – cell properties remodelled during oncogenic transformation (Hanahan and Weinberg, 2000; Hanahan and Weinberg, 2011). Given the enhancement in IP₃-mediated Ca²⁺ signalling observed in K-Ras^{G13D}-deleted HKH2 cells, we hypothesized that mitochondrial Ca²⁺ uptake would also be enhanced and contribute to greater sensitivity to death-inducing stimuli in the K-Ras^{G13D}-negative cells. The effect of K-Ras deletion upon mitochondrial Ca²⁺ uptake during IP₃-stimulated Ca²⁺ release from the ER was therefore analysed. To induce equivalent Ca²⁺ signals between cell types, and to restrict the source for mitochondrial Ca²⁺ sequestration to Ca²⁺ arising from IP₃Rs, experimental conditions were used in which a maximal concentration of ATP was applied and cells were imaged in Ca²⁺-free imaging buffer. Mitochondrial matrix Ca²⁺ was measured by confocal imaging of mitochondrially compartmentalized rhod-2 AM (Fig. 6A). Cytoplasmic Ca²⁺ responses were detected by measuring the residual non-compartmentalized rhod-2 fluorescence in the nucleus. In this way, a mitochondrial-free region of the cell can be analysed and used as a surrogate for bulk cytosolic Ca²⁺ (Collins et al., 2001;

Fig. 3. Ca²⁺ responses induced by histamine and IP₃ ester are enhanced in the K-Ras^{G13D}-deleted HKH2 cell line. (Ai) Representative Ca²⁺ traces of HCT116 and HKH2 cells exposed to 1 μM histamine. Histamine was applied in the Ca²⁺-free imaging buffer. (Aii) Percentage of responding cells. (Aiii) Peak amplitude of Ca²⁺ response. (Aiv) AUC of responding cells. Results are means±s.e.m. of data from 4 days of experiments, where three coverslips per cell type were imaged on each day (n=12). At least 30 cells per coverslip were analysed. (Bi) Representative Ca²⁺ traces of HCT116 and HKH2 cells exposed to IP₃ ester (10 μM). (Bii) Percentage of responding cells. (Biii) Peak amplitude of Ca²⁺ response. (Biv) AUC of responding cells. Results are means±s.e.m. of data from 4 days of experiments, where three coverslips per cell type were imaged on each day (n=12). At least 60 cells per coverslip were analysed. **P<0.01; ***P<0.001 (Student's t-test).

ITPR1) expression reduced in the HKH2 K-Ras^{G13D}-deleted cells when compared to HCT116 cells (Fig. 5E). IP₃R2 (also known as ITPR2) expression was not detectable in either cell type (supplementary material Fig. S1).
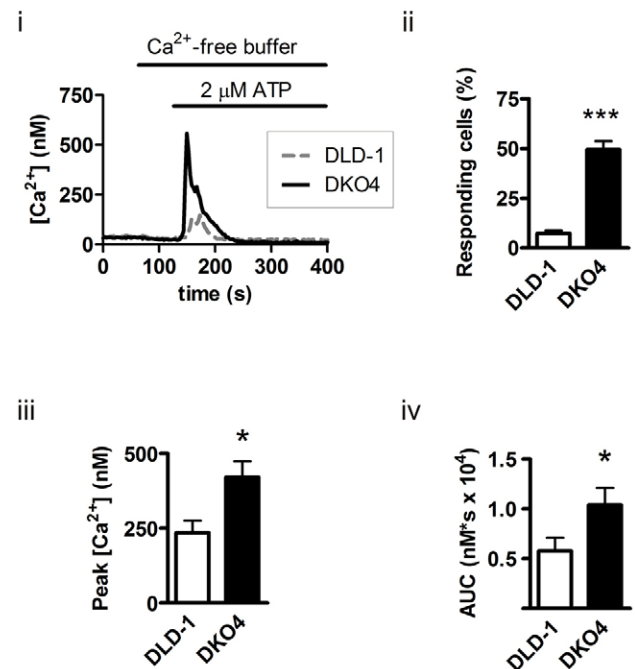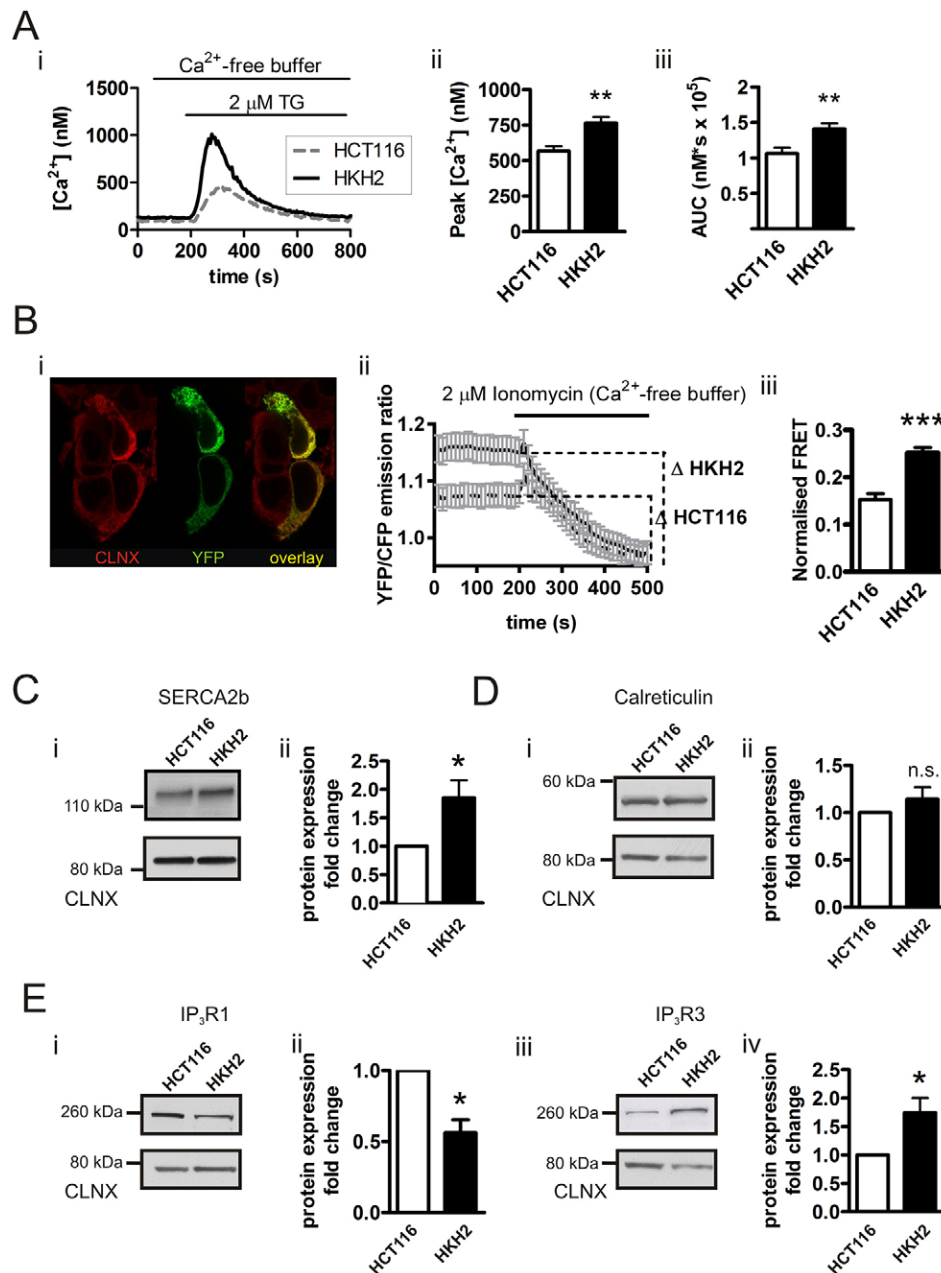
Fig. 5. ER Ca²⁺ levels are greater and expression of ER Ca²⁺-handling proteins is remodelled in K-Ras^G13D-deleted HKH2 cells. (Ai) Representative Ca²⁺ responses in HCT116 and HKH2 cells following application of thapsigargin in Ca²⁺-free imaging buffer. (Aii) Peak Ca²⁺ response. (Aiii) AUC. Results are means±s.e.m. of data from 4 days of experiments, where three coverslips per cell type were imaged on each day (*n*=12). At least 60 cells per coverslip were analysed. (Bi) Expression of the D1ER Ca²⁺ sensor in the ER. The expression and localization of D1ER determined by its excitation of YFP (in green) colocalizes with the ER-localized protein calnexin (in red; overlay image in yellow). (Bii) Representative FRET signals of D1ER-transfected cells. The Ca²⁺ level at the beginning of the experiment (represented by the YFP:CFP emission ratio) is higher in HKH2 cells compared to HCT116. (Biii) Baseline-subtracted Ca²⁺-free fluorescence of the two cell types imaged. Results are means±s.e.m. of 3 days of experiments, where three coverslips per cell type were imaged on each day (*n*=9). At least 10 D1ER-expressing cells per coverslip were analysed. *$P<0.05$; **$P<0.01$; ***$P<0.001$ (Student's *t*-test). (Ci) Representative immunoblot of SERCA2b. Calnexin (CLNX) was used as a loading control. (Cii) Fold change in SERCA2b expression in HKH2 cells with respect to HCT116 cells. Results are means±s.e.m. (*n*=21 for SERCA2b). (Di) Representative immunoblot of calreticulin. (Dii) Fold change in calreticulin protein expression in HKH2 cells with respect to HCT116 cells (mean±s.e.m., *n*=8). (Ei, Eiii) Representative immunoblot of IP₃Rs detected with an anti-IP₃R1 antibody (Ei) and an anti IP₃R3 antibody (Eiii). IP₃R2 was not expressed in the cells. Calnexin (CLNX) was used as a loading control. (Eii, Eiv). Fold change in IP₃R1 (Eii, *n*=15) and IP₃R3 (Eiv, *n*=27) expression in HKH2 cells with respect to HCT116 cells. *$P<0.05$; **$P<0.01$ (one-sample Student's *t*-test).

Szado et al., 2008). ATP induced an increase in Ca²⁺ in the majority of mitochondria of both cell types, and this remained elevated for the duration of the recording (Fig. 6Bi). Although a minor difference in the percentage of responding mitochondria was observed between cell types (Fig. 6Bii), the integrated Ca²⁺ response of the K-Ras-deleted HKH2 cells was significantly greater than in HCT116 cells (Fig. 6Biii).

Experiments were then performed to determine whether the differences in the mitochondrial Ca²⁺ uptake between the two cell types were a consequence of altered IP₃ signalling in ER–mitochondrial microdomains or due to an intrinsic alteration in the Ca²⁺ uptake properties of the mitochondria. To this end, mitochondrial Ca²⁺ uptake during the increase in cytosolic Ca²⁺ associated with store-operated Ca²⁺ influx was also monitored. Ca²⁺ influx was initiated by re-addition of Ca²⁺ to the imaging buffer following depletion of intracellular ER Ca²⁺ stores with Tg in Ca²⁺-free imaging buffer (Collins et al., 2001; Giacomello

et al., 2010; Hanson et al., 2008b). Under these conditions, a minor difference in the percentage of responding mitochondria was observed and no difference in the integrated Ca²⁺ response of mitochondria was observed between HCT116 and HKH2 cells (Fig. 6C). These observations are consistent with the reported properties of Ca²⁺ uptake from bulk cytosol rather than from the microdomains of high Ca²⁺ at the ER–mitochondrial interface (Collins et al., 2001; Giacomello et al., 2010; Hanson et al., 2008b). Together these data indicated that ER–mitochondrial Ca²⁺ flux is enhanced as a result of K-Ras^G13D deletion in a manner independent of an alteration in the intrinsic Ca²⁺ uptake properties of the mitochondria.

As a measure of the functional consequences of enhanced ER–mitochondrial Ca²⁺ flux following K-Ras^G13D deletion, the sensitivity of HCT116 and HKH2 cells to apoptosis induced by a stimulus that acts via Ca²⁺ was assessed. We and others have previously shown that menadione induces apoptosis through
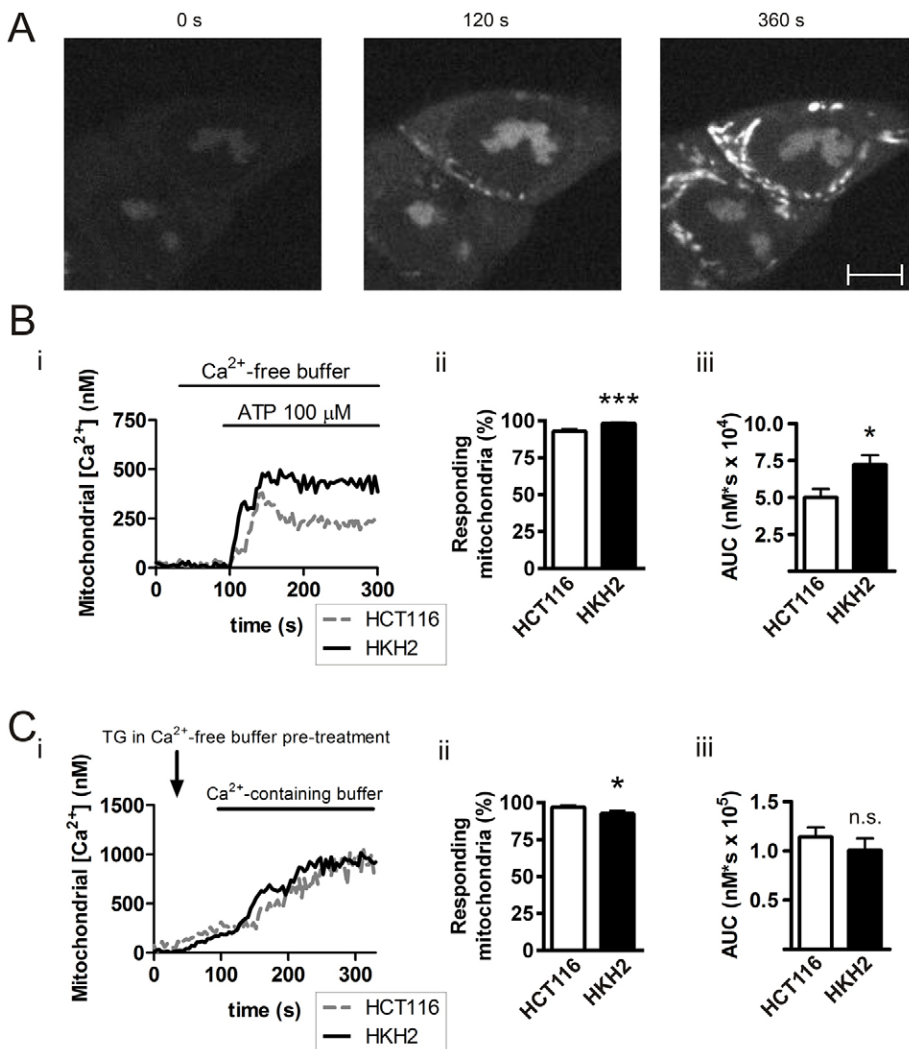
Fig. 6. Mitochondrial Ca^{2+} responses are enhanced by loss of K-Ras^{G13D} in HKH2 cells. (A) Representative images of cells exhibiting mitochondrial Ca^{2+} responses to 100 µM ATP. Experiments are in Ca^{2+}-free imaging buffer. Time points of experiments are indicated. Scale bar: 10 µm. (Bi) Representative traces of mitochondrial Ca^{2+} responses in cells exposed to 100 µM ATP in the absence of extracellular Ca^{2+}. (Bii) Percentage of responding mitochondria. (Biii) AUC of mitochondrial Ca^{2+} response. (Ci) Representative mitochondrial Ca^{2+} responses during store operated Ca^{2+} entry, which was initiated by addition of Ca^{2+} to the imaging buffer following depletion of intracellular stores with Tg (arrow). (Cii) Percentage of mitochondria exhibiting Ca^{2+} responses. (Ciii) AUC of mitochondrial Ca^{2+} response. All bar graphs represent the means±s.e.m. of data from 3 days of experiments, where three coverslips per cell type were imaged on each day. At least ten cells per coverslip and at least five mitochondria per cell were analysed. *$P<0.05$; **$P<0.01$; ***$P<0.001$; n.s., not significant (Student's t-test).

reactive oxygen species (ROS)-dependent activation of IP$_3$Rs and an elevation in mitochondrial Ca^{2+} (Baumgartner et al., 2009; Szado et al., 2008). To this end, cytochrome c loss from mitochondria and DNA fragmentation were used as hallmarks of apoptosis. Cytochrome c distribution was assessed by confocal imaging of cells immunolabelled with antibodies against cytochrome c following exposure to menadione for 20 h (Fig. 7Ai). Although untreated HKH2 and HCT116 cells displayed a typical mitochondrial distribution of cytochrome c, this mitochondrial distribution was lost following treatment with menadione and became distributed diffusely throughout the cytosol (Fig. 7Ai). HKH2 cells however exhibited a greater sensitivity to menadione treatment than HCT116 cells with cytochrome c being lost from the mitochondria in a significantly greater number of cells at 50 µM menadione (Fig. 7Aii). DNA fragmentation was assessed as the percentage of the cell population with DNA content lower than that observed in the G1 phase of the cell cycle. DNA content was determined by flow cytometric analysis of cells stained with propidium iodide (PI) (Hanson et al., 2008a). Basal levels of cell death were detected in both HCT116 and HKH2 cells (Fig. 7B). Application of menadione induced apoptosis in both HCT116 and HKH2 cells. However, the percentage of the menadione-treated cell population

with DNA content lower than in G1 phase was significantly greater in the K-Ras^{G13D}-deleted cells than in their HCT116 counterparts (Fig. 7B). Caspase activation, a further hallmark of apoptosis, was also observed following menadione treatment in HCT116 and HKH2 cells by imaging (Fig. 7Ai) and immunoblotting (supplementary material Fig. S2).

Taken together, these data indicate that decreased flux of Ca^{2+} to the mitochondria contributes to the oncogenic phenotype of HCT116 cells.

DISCUSSION
The impact of oncogenic K-Ras on Ca^{2+} signals, particularly in the context of oncogenic transformation is poorly understood. Here, we provide the first demonstration of an interaction of natively expressed oncogenic K-Ras with Ca^{2+} signalling and how this signalling crosstalk might affect cell fate. By comparing isogenic colon cancer cell line pairs expressing either a single copy of mutant K-Ras^{G13D} or no mutant K-Ras we have determined that K-Ras^{G13D} deletion enhances IP$_3$-dependent Ca^{2+} signals and ER–mitochondrial Ca^{2+} flux and that this sensitizes cells to pro-apoptotic stimuli. From these data, we propose that suppression of IP$_3$ signalling from the ER and Ca^{2+} uptake by the mitochondria contributes to the pro-survival
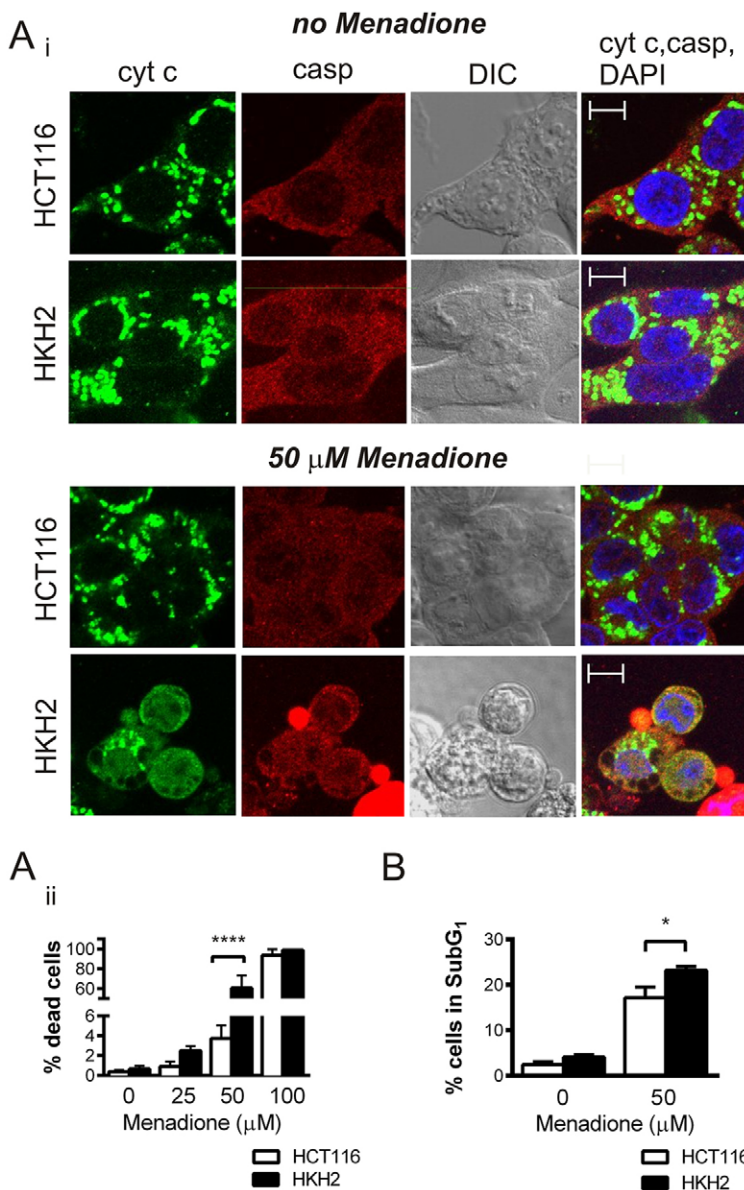
Fig. 7. Sensitivity to apoptosis induced by menadione is enhanced by loss of K-Ras^{G13D} in HKH2 cells. (Ai) Confocal images of cytochrome c (green) and activated caspase 3 (red) in HCT116 and HKH2 cells following 20 h exposure to 50 μM menadione. Scale bar: 10 μm. (Aii) Number of cells exhibiting diffuse cytochrome c. Upon treatment with menadione, a higher percentage of HKH2 cells displayed diffuse cytochrome c distribution in comparison with HCT116 (n=3 experiments). (B) Effect of exposure to menadione for 20 h upon the percentage of HCT116 and HKH2 cells with a DNA content lower than in the G1 phase (Sub-G$_1$). DNA content was measured by flow cytometric analysis of PI-stained DNA. Results are means±s.e.m. (n=5). *P<0.05 (two-way ANOVA).

properties of K-Ras^{G13D} associated with the oncogenic phenotype.

Cytosolic Ca^{2+} signals are generated by Ca^{2+} entry across the plasma membrane, Ca^{2+} release from intracellular stores or a combination of both (Berridge et al., 2003; Berridge et al., 2000; Bootman et al., 2003). Through manipulation of these Ca^{2+} signalling pathways in transformed cells, specific roles for each of these Ca^{2+} sources in controlling aspects of cancer cell biology including regulation of cell proliferation, migration and death have been described (Crépin et al., 2007; Humez et al., 2004; Legrand et al., 2001; Lipskaia et al., 2009; Szatkowski et al., 2010; Yoshida et al., 2012). Altered expression of a number of Ca^{2+}-handling proteins in tumour tissue has also been determined (Arbabian et al., 2012; Korosec et al., 2006; Monteith et al., 2012; Monteith et al., 2007; Motiani et al., 2013). Although these findings are suggestive of an important role of certain Ca^{2+} signalling pathways in transformed cells, causality has not been demonstrated. However, somatic mutations in the gene encoding SERCA have been identified in patients with colon cancer leading to the proposal that altered Ca^{2+} signalling

predisposes to oncogenic transformation (Korosec et al., 2006). Cancers arise through mutations in oncogenes such as *KRAS* or tumour suppressors that serve to promote or suppress the activity of the proteins they encode, respectively (Hanahan and Weinberg, 2000). How the native expression of a specific oncoprotein in transformed cells affects Ca^{2+} signalling and whether this contributes to the phenotype of the transformed cell is, however, not clear. A particular issue when investigating Ca^{2+} signalling pathways is that the analysis of Ca^{2+} signalling is only possible in live cells. The availability of appropriate controls for the cell line expressing the driving oncogene is also essential (Roderick and Cook, 2008). For analysing the effects of activated Ras isoforms, this is a particular concern because oncogenic K-Ras can induce senescence or cell proliferation depending on the level of overexpression (Serrano et al., 1997; Tuveson et al., 2004). These issues are minimized through the use of isogenic cell line pairs in which studies are performed upon a cancer cell line harbouring a single allele of an activating oncogene and a second cell line in which the driving oncogene has been deleted by homologous recombination (Shirasawa et al., 1993). By

comparing hormone-agonist-induced Ca^{2+} signalling between such pairs of cell lines, we found that loss of K-Ras^{G13D} enhanced cytosolic Ca^{2+} signals. The elevated Ca^{2+} responses in K-Ras^{G13D}-deleted cells persisted in Ca^{2+}-free imaging buffer, indicating that Ca^{2+} release from the ER was important in defining the properties of the Ca^{2+} response. Importantly, Ca^{2+} signals were greater in two different colorectal cancer cell lines in which K-Ras^{G13D} had been deleted (HKH2 and DKO4), as well as in HCT116 cells when K-Ras expression was reduced by siRNA, indicating that suppression of hormone-stimulated Ca^{2+} signalling is a common response to K-Ras^{G13D} in colorectal cell lines.

The greater magnitude of hormone-induced Ca^{2+} release from the ER in K-Ras^{G13D}-deleted cells could have arisen through a number of mechanisms. For example, by increased GPCR expression or coupling to downstream effectors, modification in inositol phosphate metabolism, changes in IP$_3$R expression or through a greater Ca^{2+} content of the ER. Given its pleiotropic nature, we speculated that Ras could interfere with any or all of these processes. Increased PLC activity and IP$_3$ levels have been reported in a number of transformed cell lines and in breast, ovarian and colonic carcinoma, suggesting that basal signalling is enhanced as a result of transformation (Weber, 2005). Oncogenic K-Ras might also increase signalling activity through stimulating PLCε, which in turn, by increasing IP$_3$ levels, would promote Ca^{2+} release from stores (Kelley et al., 2001). However, our observations that Ca^{2+} signals are negatively correlated with Ras abundance suggests that enhanced basal signalling possibly involving PLCε does not contribute to Ras-mediated regulation of Ca^{2+} signalling in cells harbouring mutated K-Ras^{G13D}. As Ca^{2+} signals induced by stimulation of the histamine receptor, another GPCR, were also greater in K-Ras^{G13D}-deleted cells, it is unlikely that modifications in purinergic receptor expression contributed to the effects of K-Ras^{G13D} deletion. Similarly, Ca^{2+} responses induced by a cell-permeant analogue of IP$_3$ were greater in K-Ras^{G13D}-deleted cells than in the isogenic parental cell line. As this cell-permeant IP$_3$ directly activates IP$_3$Rs, circumventing GPCRs, G proteins and PLC, our data indicate that native levels of K-Ras^{G13D} has a direct effect on IP$_3$R-mediated Ca^{2+} release from the ER.

Notably, although the combined expression of IP$_3$R isoforms was unaltered by K-Ras^{G13D} deletion, the relative abundance of the expressed IP$_3$R subtypes was altered in the K-Ras^{G13D}-deleted cells. In particular, in K-Ras^{G13D}-deleted cells, IP$_3$R3 expression was increased and IP$_3$R1 expression suppressed, indicating that in colorectal cancer cell lines, K-Ras^{G13D} represses IP$_3$R3 expression. Changes in the expression of IP$_3$Rs in cancer cells have been reported previously. Most notably, an increase in IP$_3$R3 expression at the mRNA level has been detected in a recent microarray analysis of K-Ras-deleted cells lines (Vartanian et al., 2013). In gastric cancer cells, an increase in IP$_3$R3 was observed in the ascites, but not in cancer cells established from primary tumours. In the ascites, IP$_3$R3 inhibition by 2-aminoethoxydiphenyl borate (2-APB) induced apoptosis (Sakakura et al., 2003). IP$_3$R3 expression is also increased in MCF-7 cells induced to proliferate with estradiol (Szatkowski et al., 2010). An increase in IP$_3$R2 expression together with K-Ras has been observed in non-small cell lung cancer (NSCLC) cells (Heighway et al., 1996). Given the differing properties of each IP$_3$R isoform, this change in isoform composition following K-Ras deletion might have important consequences. As different IP$_3$R isoforms are regulated differently by IP$_3$ and Ca^{2+}, giving

rise to distinct Ca^{2+} signalling fingerprints (Hattori et al., 2004; Miyakawa et al., 1999), the change in the relative abundance of each IP$_3$R isoform could contribute to the differences in Ca^{2+} signalling observed between the two cell types. A notable feature of IP$_3$R3 is that it is least sensitive to Ca^{2+}-dependent inhibition (Hagar et al., 1998). As a result, whereas expression of IP$_3$R1 supports regular Ca^{2+} oscillations, monophasic Ca^{2+} transients are observed in IP$_3$R3-expressing cells (Almirza et al., 2010; Hattori et al., 2004; Miyakawa et al., 1999). Indeed, siRNA reduction in IP$_3$R3 expression in MCF-7 breast cancer cells transformed Ca^{2+} responses from a peak–plateau to a more oscillatory profile (Szatkowski et al., 2010). These different Ca^{2+} signatures probably allow signalling from each receptor to participate in different cell fate choices. Ca^{2+} oscillations arising from IP$_3$R1 might be optimized for controlling cytokinesis (Kittler et al., 2004) and gene expression (Dolmetsch et al., 1998), whereas the sustained Ca^{2+} signals arising from IP$_3$R3 might promote cell death (Blackshaw et al., 2000; Khan et al., 1996; Mendes et al., 2005; Szatkowski et al., 2010). Thus, a potential outcome of these different Ca^{2+} signatures is that the Ca^{2+} oscillations that arise from IP$_3$R1 in HCT116 cells sustain their rapid proliferation, whereas the reduction in IP$_3$R3 protects the cells from cytotoxic Ca^{2+} signals.

An increase in ER Ca^{2+} store content was also observed in K-Ras^{G13D}-deleted cells. As the Ca^{2+} content of the ER is a dominant determinant of the magnitude of the IP$_3$-stimulated Ca^{2+} transient (Berridge, 2006; Caroppo et al., 2003), it is likely that this alteration in ER Ca^{2+} store content contributes substantially to the enhancement in Ca^{2+} signalling observed in K-Ras^{G13D}-deleted cells. Our data are consistent with the view that a relatively low level of Ca^{2+} in the ER offers an advantage to the transformed cell (Bergner and Huber, 2008). Specifically, by limiting Ca^{2+} release, the effect of stimuli that serve to induce apoptosis is diminished. The cytotoxic effects of Ca^{2+} release from the ER are mediated through accumulation in mitochondria, which results in permeability transition and activation of apoptotic pathways (Pinton et al., 2008; Roderick and Cook, 2008). Elevated Ca^{2+} also activates DNA endonucleases, promotes phosphatidylserine exposure, leads to cellular ATP depletion, and increases ROS and ER stress (Orrenius et al., 2003). Despite this well-accepted view of the benefit of lower ER Ca^{2+} for survival of transformed cells, much of the supporting data has emerged through investigation into the mechanism of actions of proteins involved in regulation of cell death pathways that are dysregulated in cancer. For example, enhanced expression of Bcl-2 family members or knockout of BH3-only pro-apoptotic proteins (which result in increased abundance of the anti-apoptotic family members) result in a lowering of free ER Ca^{2+} levels and reduced flux of Ca^{2+} to the mitochondria (Pinton et al., 2008; Roderick and Cook, 2008). By increasing leak through the IP$_3$R or suppressing their activity, Bcl-2 family members also reduce IP$_3$-induced Ca^{2+} release (Chen et al., 2004; Oakes et al., 2005). No differences in the expression of Bak, Bax, Bcl-2, Bcl-XL or Mcl-1 was detected between the HCT116 and HKH-2 cell types analysed here (data not shown). Notably, when analysed in HCT116 cells, no prominent role for Bax in mitochondrial outer membrane permeabilization (MOMP) was detected (De Marchi et al., 2004), supporting the hypothesis that Ca^{2+} signalling remodelling by oncogenic K-Ras activation in HCT116 cells does not involve alterations in the expression of Bcl-2 family members. IP$_3$R activity is also reduced by phosphorylation by the pro-survival kinase PKB/Akt (Khan

et al., 2006; Marchi et al., 2012; Szado et al., 2008); a kinase that is increased in activity in many cancers.

A decrease in ER Ca^{2+} content has been detected in a subset of lung cancer cell lines when compared to normal human bronchial epithelial cells (Bergner et al., 2009). Consistent with the reduction in ER Ca^{2+} in cancer, a reduction in expression of SERCA pump has been observed in cancer-derived cell lines and in tumours. Mutations in SERCA that result in loss of expression or activity have also been detected in tumours (Monteith et al., 2007). The importance of SERCA expression is also demonstrated by the induction of squamous cell cancers in SERCA2b haploinsufficient mice (Prasad et al., 2005). In humans, however, loss of one SERCA allele results in Darrier's disease, which is characterized by a skin phenotype (Hovnanian, 2007). In line with these studies, SERCA2b expression was significantly increased in K-Ras^{G13D}-deleted cells, showing that a reduction in SERCA2b activity contributes to the phenotype of K-Ras-transformed cells. The increase in ER Ca^{2+} in K-Ras^{G13D}-deleted cells might also be explained by the observed reduction in IP$_3$R1, which has been reported to contribute to the Ca^{2+} leak from the ER (Kasri et al., 2006; Oakes et al., 2005). A positive correlation between ER Ca^{2+} levels and proliferation has been observed in prostate cancer cell lines (Legrand et al., 2001). However, because depletion of the ER Ca^{2+} store inhibits proliferation and induces cell death in transformed cells, it would be important to correlate the absolute Ca^{2+} content of the ER and cell proliferation in these studies.

The mitochondria are an important target of Ca^{2+} released from the ER (Rizzuto et al., 2012). Mitochondrial Ca^{2+} uptake is a low-affinity process. As such, mitochondria preferentially accumulate Ca^{2+} at sites of close apposition with the ER called mitochondrial-associated membranes (MAMs), which are enriched in Ca^{2+} release channels including IP$_3$Rs (Csordás et al., 2010; Hajnóczky and Csordás, 2010; Rizzuto et al., 2004). Through this preferred pathway, mitochondrial function, including metabolism and induction of apoptotic cell death, is acutely modulated by IP$_3$-mediated Ca^{2+} signals. Here, we show the first evidence of modifications in mitochondrial Ca^{2+} uptake downstream of endogenous oncogenic K-Ras. The ablation of oncogenic K-Ras^{G13D} increased the accumulation of Ca^{2+} in the mitochondria following Ca^{2+} release from the ER. Notably, the difference between the HCT116 and HKH2 cells was lost when Ca^{2+} uptake during Ca^{2+} influx from the extracellular space was analysed. Under these conditions, Ca^{2+} uptake into the mitochondria is not restricted to the IP$_3$R-containing MAMs. As such, microdomains of high Ca^{2+} at the ER–mitochondrial interface do not drive mitochondrial Ca^{2+} sequestration and the uptake observed is due to the properties of the mitochondrial uptake mechanisms alone (Collins et al., 2002; Rizzuto and Pozzan, 2006; Szabadkai and Duchen, 2008). Our data therefore suggest that the enhancement of ER–mitochondrial Ca^{2+} flux following K-Ras^{G13D} ablation is through modification of IICR. Consistent with increased IICR, this enhanced ER-to-mitochondria Ca^{2+} flux in HKH2 cells was mirrored by an increased sensitivity of these cells to Ca^{2+}-induced cell death. The increase in the ER-to-mitochondria Ca^{2+} transfer observed in HKH2 cells indicates that the expression of K-Ras^{G13D} acts to reduce this flux in HCT116 cells. In line with their lower ER–mitochondrial Ca^{2+} flux and apoptosis, the expression of IP$_3$R3, which has been proposed to specifically mediate pro-apoptotic Ca^{2+} fluxes at the MAM, is also reduced in HCT116 cells (Blackshaw et al., 2000; Khan et al., 1996; Mendes et al., 2005).

More recently, the tumour suppressor PML, which is localized at the ER, has been reported to specifically mediate the dephosphorylation of IP$_3$R3 by PP2a (Giorgi et al., 2010). Notably, the reintroduction of ER-targeted PML in PML$^{-/-}$ cells restored the sensitivity to Ca^{2+}-dependent apoptosis (induced by Menadione and H_2O_2), but not that to Ca^{2+}-independent apoptosis (induced by the DNA-damaging agent Etoposide) (Giorgi et al., 2010). This finding is consistent with the increased sensitivity to menadione observed in the K-Ras^{G13D}-ablated HKH2 cells.

In conclusion, our data describes for the first time the alterations in Ca^{2+} regulation driven by a single oncogenic K-Ras^{G13D} allele in colorectal cells. The enhancement of Ca^{2+} handling, mitochondrial sequestration and cell death as a result of loss of K-Ras^{G13D} in two isogenic models indicates that suppression of Ca^{2+} signalling is a common response to K-Ras^{G13D}. Owing to its pleiotropic actions, modulation by K-Ras^{G13D} in colorectal cells is likely also to contribute to other aspects of cell physiology that serve to promote cell transformation including enhancement of cell proliferation or modulation of metabolism. The importance of Ras activation and downstream pathways in cancers where mutated Ras is not the primary cause, such as mutations in EGFR or B-Raf, raises the possibility that the modulation of Ca^{2+} fluxes observed in this study due to K-Ras^{G13D} is a common feature of many cancers and is thus a target for intervention.

MATERIALS AND METHODS
Cell culture
HCT116 and DLD-1 cells (both K-Ras$^{G13D/WT}$) and their respective isogenic derivatives HKH2 and DKO4 (both K-Ras$^{-/WT}$) were a kind gift of Senji Shirasawa (Fukuoka University, Japan) and have been previously described (Shirasawa et al., 1993). Cells were cultured in Dulbecco's modified Eagle's medium (DMEM; Life Technologies, Carlsbad, CA, USA), containing 10% heat-inactivated fetal bovine serum (FBS) (Invitrogen), 1% penicillin/streptomycin solution (5 units penicillin, 55 µg streptomycin) (Sigma, Dorset, UK). Cells were maintained at 37℃ under 5% CO_2 in saturated humidity and were passaged upon reaching 80–90% confluency. Coverslips were coated with poly-L-lysine prior to seeding of cells.

siRNA transfection
siGENOME SMART Pool for K-Ras and siGENOME non-targeting control oligonucleotides (Dharmacon, Thermo) were reverse transfected using Dharmafect-2 transfection reagent (Dharmacon, Thermo) according to the manufacturer's instructions. Briefly, 2×10^5 cells in a 12-well dish or 4×10^5 cells in a 6-well dish were transfected with siRNAs at a final concentration of 25 nM. The medium overlying the cells was exchanged after 24 h, and protein expression measured and Ca^{2+} imaging experiments performed after a further 24 h.

Imaging of cytosolic Ca^{2+}
Cytosolic Ca^{2+} was imaged as previously described (Peppiatt et al., 2003). Briefly, cells were seeded onto poly-L-lysine-coated coverslips at equivalent densities and imaged after 48 h. Prior to each experiment, coverslips were mounted into stainless steel imaging chambers and loaded with fura-2 AM (Life Technologies; 2 µM for 30 min, followed by de-esterification in imaging buffer for a further 30 min). Coverslips were imaged on the stage of a Nikon Eclipse TE200 inverted epifluorescence microscope equipped with a Nikon PlanFluor 20×/ 0.75 NA multi immersion objective (Nikon, Kingston Upon Thames, Surrey, UK). Excitation light at 340 and 380 nm was selected using a motorized filter wheel (Sutter Industries, Novato, CA, USA) at a frequency of 1 image pair every 3 s with an exposure of 200 ms, and emitted light was selected using a 400 nm dichroic mirror and filtered through a 460 nm long pass filter. Images were captured using a Hamamatsu ORCA ER charge-coupled device (CCD) camera. Three coverslips per cell type were imaged per day on three

separate days, each coverslip containing at least 50 cells. Ca^{2+} concentration was calculated according to Grynkiewicz et al. (Grynkiewicz et al., 1985).

Imaging of ER Ca^{2+}

The FRET-based, genetically-encoded D1ER Ca^{2+} indicator was a kind gift of Amy Palmer (University of Colorado, Boulder, USA). The affinity of the indicator for Ca^{2+} has been determined to be 60 µM, allowing its successful use to monitor resting and dynamic changes in ER luminal $[Ca^{2+}]$ (Palmer et al., 2004). In experiments involving D1ER, cells were seeded as indicated for ratiometric imaging but transfected with the D1ER construct after 24 h using JetPei (PolyPlus Transfection, Ilkirch, France) according to manufacturer's specification. Cells were imaged at 24 h post transfection. Coverslips were mounted in stainless steel chambers and imaged on the stage of an Olympus IX81 inverted microscope equipped with an Olympus UPlanSApo 20×/0.75 NA air objective. Excitation light at 435/10 nm was selected using a Polychrome V monochromator (Olympus, Southend-on-Sea, UK). Emitted fluorescence of CFP and YFP was simultaneously captured using a Cairn Optosplit II image splitter (Cairn Research Limited, Graveney Road, Faversham Kent). The image splitter unit was configured with a 515 nm dichroic mirror, which reflected the emitted fluorescence of CFP (further filtered through a 485/40 nm band-pass filter), and passed the emission of YFP (further filtered through a 535/30 nm band-pass filter).

Imaging of mitochondrial Ca^{2+}

Mitochondrial Ca^{2+} was imaged as previously described using rhod-2 AM as a Ca^{2+} indicator (Szado et al., 2008). Prior to each experiment, cells were loaded with rhod-2 AM (4 µM for 30 min at room temperature followed by de-esterification in imaging buffer for a further 30 min). Cells were imaged using a VisiTech VoxCell Scan spinning disc confocal configured on a Nikon TE2000 microscope equipped with a Nikon 60×/1.25 NA oil immersion objective. Rhod-2 was excited by illumination with the 568 nm line of an argon/krypton laser. Emitted fluorescence was filtered through a 575/50 nm band-pass filter. Images were captured using a Hamamatsu ORCA ER CCD camera controlled by the Visitech Voxcell Scan software. Ca^{2+} concentration was calculated as previously described (Collins et al., 2001).

Immunoblotting

Cells were harvested 48 h post seeding and protein lysate was quantified using a bicinchoninic acid (BCA) protein assay kit (Thermo Scientific). An equivalent amount of each sample (15 to 50 µg) was loaded onto 7% self-poured polyacrylamide gels or onto 4–12% gradient pre-cast gels (NUPAGE; Life Technologies). Proteins were transferred from the gels onto polyvinilidene fluoride (PVDF) membranes (for IP_3Rs and SERCAs and their loading controls) or nitrocellulose. Non-specific protein-binding sites were first blocked by incubation for 1 h in TBS containing 0.05% Tween 20 (TBS-T) and 5% milk. Membranes were subsequently probed with primary antibodies (diluted as indicated below in TBS-T milk) for 1 h at room temperature or 4°C overnight. Details of primary antibodies are as follows: anti-K-Ras (dilution 1:500, AbdSerotec); anti-SERCA2b [dilution 1:1000, kind gift of Frank Wuytack, University of Leuven (Wuytack et al., 1989)]; anti-IP_3R3 (dilution 1:1000, BD Biosciences); anti-IP_3R1 [dilution 1:1000, in-house generated (Kasri et al., 2004)]; anti-calnexin (dilution 1:20,000, Sigma); anti-SERCA3 [dilution 1:1000, gift of Frank Wuytack (Wuytack et al., 1994)]; anti-IP_3R2 [dilution 1:500, in-house generated (Harzheim et al., 2009)]; anti-calreticulin (1:1000; Roderick et al., 1997); anti-active caspase 3 (1:1000, BD BioSciences); anti-GAPDH (1:5000, Sigma) and anti-β actin (1:5000, AbCam). Excess antibodies were removed by washing with TBS-T. Membranes were then probed with either horseradish peroxidase (HRP)-conjugated (Jackson Immunoresearch; 1:10,000 dilution) or fluorescently-labelled secondary antibodies (Life Technologies and LI-COR; both at 1:5000). All membranes were then washed in five exchanges of TBS-T and one of TBS before band detection. HRP-conjugated antibodies were detected by chemiluminescence (ECL) (Thermo Scientific) and subsequent exposure to film, and fluorescently-labelled secondary antibodies (Life Technologies and LI-COR) were detected by digital scanning (LI-COR Odyssey). For band quantification, intensity values were obtained either through analysis of digitized film (ImageJ, for ECL detection) or Image Studio (for LI-COR detection). Bands of the protein of interest were normalized against the corresponding loading control band. Following normalization, protein abundance in the experimental conditions of interest was normalized to the control.

Immunofluorescence

Immunofluorescence was performed as previously described (Higazi et al., 2009). Briefly, at 48 h post seeding, cells were fixed with fixation buffer (2% paraformaldehyde, 0.05% glutaraldehyde in PBS) and permeabilized with 0.2% Triton X-100 in PBS. After incubation in blocking solution (0.1% Triton X-100, 5% donkey goat serum diluted in PBS), cells were probed with primary antibodies (diluted in blocking solution) for 1 h at room temperature. Details of primary antibodies are as follows: anti-cytochrome c (dilution 1:200, Santa Cruz Biotechnology); and anti-active caspase 3 (1:200, BD BioSciences); anti-calnexin (1:500, Sigma). After removal of excess antibodies by washing in 0.1% Triton X-100 in PBS, cells were incubated with Alexa-Fluor-labelled secondary antibodies (Life Technologies) for 1 h at room temperature. Excess antibody was subsequently removed with five washes in 0.1% Triton X-100 in PBS and two washes in PBS. Coverslips were mounted in Vectashield containing DAPI, which also counterstained nuclei. Cells were imaged by point-scanning confocal microscopy using appropriate laser lines for excitation of the dyes (Olympus FV1000 confocal configured on an Olympus IX81 inverted microscope using a 60×/1.35 NA oil immersion objective for calnexin and YFP imaging, and a Nikon A1R confocal configured on a Nikon Ti inverted microscope and using 60×/1.4 NA oil immersion objective for imaging of cytochrome c and activated caspase). Images were processed and analysed using Image J.

Cell cycle analysis

Cells in the medium were collected and then pooled with cells that remained attached to their substrate that were harvested by trypsinization. After washing in PBS, cells were fixed with 70% ethanol prior to RNase treatment and staining with propidium iodide (PI). Stained cells were analysed with a Becton Dickinson FACSCalibur flow cytometer (Oxford, UK). Single cells in suspension were excited at 488 nm by an argon laser and analysed according to the intensity of emitted fluorescence through a 585/42 band pass filter (Hanson et al., 2008a).

Menadione treatment of cells

At 24 h post seeding, cells were exposed to menadione diluted in culture medium at concentrations between 25 and 100 µM. Control samples cultured in parallel were also analysed. Cells were harvested 20 h after exposure to menadione and processed for flow cytometric analysis or immunofluorescence.

Statistical analysis

Where data was compared to normalized control a one-sample Student's t-test was employed. Other experiments were analysed by Student's t-test or two-way ANOVA. Significance was accepted at $P<0.05$.

Competing interests

The authors declare no competing interests.

Author contributions

C.P., T.C.F. and H.L.R. performed experiments and analysed data. C.P., M.D.B., S.J.C. and H.L.R. conceived of the study and interpreted data. C.P., S.J.C. and H.L.R. prepared the manuscript.

Supplementary material

Supplementary material available online at
http://jcs.biologists.org/lookup/suppl/doi:10.1242/jcs.141408/-/DC1

References

Almirza, W. H., Peters, P. H., van Meerwijk, W. P., van Zoelen, E. J. and Theuvenet, A. P. (2010). Different roles of inositol 1,4,5-trisphosphate receptor subtypes in prostaglandin F(2alpha)-induced calcium oscillations and pacemaking activity of NRK fibroblasts. *Cell Calcium* **47**, 544-553.

Arbabian, A., Brouland, J. P., Apati, A., Paszty, K., Hegedus, L., Enyedi, A., Chomienne, C. and Papp, B. (2012). Modulation of endoplasmic reticulum calcium pump expression during lung cancer cell differentiation. *FEBS J.* **280**, 5408-5418.

Barbacid, M. (1987). ras genes. *Annu. Rev. Biochem.* **56**, 779-827.

Baumgartner, H. K., Gerasimenko, J. V., Thorne, C., Ferdek, P., Pozzan, T., Tepikin, A. V., Petersen, O. H., Sutton, R., Watson, A. J. and Gerasimenko, O. V. (2009). Calcium elevation in mitochondria is the main Ca2+ requirement for mitochondrial permeability transition pore (mPTP) opening. *J. Biol. Chem.* **284**, 20796-20803.

Belden, S. and Flaherty, K. T. (2012). MEK and RAF inhibitors for BRAF-mutated cancers. *Expert Rev. Mol. Med.* **14**, e17.

Bergner, A. and Huber, R. M. (2008). Regulation of the endoplasmic reticulum Ca(2+)-store in cancer. *Anticancer. Agents Med. Chem.* **8**, 705-709.

Bergner, A., Kellner, J., Tufman, A. and Huber, R. M. (2009). Endoplasmic reticulum Ca2+-homeostasis is altered in small and non-small cell lung cancer cell lines. *J. Exp. Clin. Cancer Res.* **28**, 25.

Berridge, M. J. (2006). Calcium microdomains: organization and function. *Cell Calcium* **40**, 405-412.

Berridge, M. J., Bootman, M. D. and Lipp, P. (1998). Calcium – a life and death signal. *Nature* **395**, 645-648.

Berridge, M. J., Lipp, P. and Bootman, M. D. (2000). The versatility and universality of calcium signalling. *Nat. Rev. Mol. Cell Biol.* **1**, 11-21.

Berridge, M. J., Bootman, M. D. and Roderick, H. L. (2003). Calcium signalling: dynamics, homeostasis and remodelling. *Nat. Rev. Mol. Cell Biol.* **4**, 517-529.

Blackshaw, S., Sawa, A., Sharp, A. H., Ross, C. A., Snyder, S. H. and Khan, A. A. (2000). Type 3 inositol 1,4,5-trisphosphate receptor modulates cell death. *FASEB J.* **14**, 1375-1379.

Bollag, G. and McCormick, F. (1991). Regulators and effectors of ras proteins. *Annu. Rev. Cell Biol.* **7**, 601-632.

Bootman, M. D., Roderick, H. L., O'Connor, R., Berridge, M. J. and Edward, A. D. (2003). Intracellular calcium signaling. In *Handbook of Cell Signaling*, pp. 51-56. Burlington, MA: Academic Press.

Brouland, J. P., Gélébart, P., Kovàcs, T., Enouf, J., Grossmann, J. and Papp, B. (2005). The loss of sarco/endoplasmic reticulum calcium transport ATPase 3 expression is an early event during the multistep process of colon carcinogenesis. *Am. J. Pathol.* **167**, 233-242.

Bunney, T. D. and Katan, M. (2006). Phospholipase C epsilon: linking second messengers and small GTPases. *Trends Cell Biol.* **16**, 640-648.

Bunney, T. D., Harris, R., Gandarillas, N. L., Josephs, M. B., Roe, S. M., Sorli, S. C., Paterson, H. F., Rodrigues-Lima, F., Esposito, D., Ponting, C. P. et al. (2006). Structural and mechanistic insights into ras association domains of phospholipase C epsilon. *Mol. Cell* **21**, 495-507.

Cárdenas, C., Miller, R. A., Smith, I., Bui, T., Molgó, J., Müller, M., Vais, H., Cheung, K. H., Yang, J., Parker, I. et al. (2010). Essential regulation of cell bioenergetics by constitutive InsP3 receptor Ca2+ transfer to mitochondria. *Cell* **142**, 270-283.

Caroppo, R., Colella, M., Colasuonno, A., DeLuisi, A., Debellis, L., Curci, S. and Hofer, A. M. (2003). A reassessment of the effects of luminal [Ca2+] on inositol 1,4,5-trisphosphate-induced Ca2+ release from internal stores. *J. Biol. Chem.* **278**, 39503-39508.

Chen, R., Valencia, I., Zhong, F., McColl, K. S., Roderick, H. L., Bootman, M. D., Berridge, M. J., Conway, S. J., Holmes, A. B., Mignery, G. A. et al. (2004). Bcl-2 functionally interacts with inositol 1,4,5-trisphosphate receptors to regulate calcium release from the ER in response to inositol 1,4,5-trisphosphate. *J. Cell Biol.* **166**, 193-203.

Collins, T. J., Lipp, P., Berridge, M. J. and Bootman, M. D. (2001). Mitochondrial Ca(2+) uptake depends on the spatial and temporal profile of cytosolic Ca(2+) signals. *J. Biol. Chem.* **276**, 26411-26420.

Collins, T. J., Berridge, M. J., Lipp, P. and Bootman, M. D. (2002). Mitochondria are morphologically and functionally heterogeneous within cells. *EMBO J.* **21**, 1616-1627.

Conway, S. J., Thuring, J. W., Andreu, S., Kvinlaug, B. T., Llewelyn Roderick, H. L., Bootman, M. D. and Holmes, A. B. (2006). The synthesis of membrane permeant derivatives of myo-inositol 1,4,5-trisphosphate. *Aust. J. Chem.* **59**, 887-893.

Cook, S. J. and Lockyer, P. J. (2006). Recent advances in Ca(2+)-dependent RAS regulation and cell proliferation. *Cell Calcium* **39**, 101-112.

Crépin, A., Bidaux, G., Vanden-Abeele, F., Dewailly, E., Goffin, V., Prevarskaya, N. and Slomianny, C. (2007). Prolactin stimulates prostate cell proliferation by increasing endoplasmic reticulum content due to SERCA 2b over-expression. *Biochem. J.* **401**, 49-55.

Csordás, G., Renken, C., Várnai, P., Walter, L., Weaver, D., Buttle, K. F., Balla, T., Mannella, C. A. and Hajnóczky, G. (2006). Structural and functional features and significance of the physical linkage between ER and mitochondria. *J. Cell Biol.* **174**, 915-921.

Csordás, G., Várnai, P., Golenár, T., Roy, S., Purkins, G., Schneider, T. G., Balla, T. and Hajnóczky, G. (2010). Imaging interorganelle contacts and local calcium dynamics at the ER-mitochondrial interface. *Mol. Cell* **39**, 121-132.

Cullen, P. J. and Lockyer, P. J. (2002). Integration of calcium and ras signalling. *Nat. Rev. Mol. Cell Biol.* **3**, 339-348.

Cully, M. and Downward, J. (2008). SnapShot: ras signaling. *Cell* **133**, 1292-1292 e1.

De Marchi, U., Campello, S., Szabò, I., Tombola, F., Martinou, J. C. and Zoratti, M. (2004). Bax does not directly participate in the Ca(2+)-induced permeability transition of isolated mitochondria. *J. Biol. Chem.* **279**, 37415-37422.

Dolmetsch, R. E., Xu, K. and Lewis, R. S. (1998). Calcium oscillations increase the efficiency and specificity of gene expression. *Nature* **392**, 933-936.

Downward, J. (2003a). Role of receptor tyrosine kinases in G-protein-coupled receptor regulation of ras: transactivation or parallel pathways? *Biochem. J.* **376**, e9-e10.

Downward, J. (2003b). Targeting ras signalling pathways in cancer therapy. *Nat. Rev. Cancer* **3**, 11-22.

Drawnel, F. M., Wachten, D., Molkentin, J. D., Maillet, M., Aronsen, J. M., Swift, F., Sjaastad, I., Liu, N., Catalucci, D., Mikoshiba, K. et al. (2012). Mutual antagonism between IP(3)RII and miRNA-133a regulates calcium signals and cardiac hypertrophy. *J. Cell Biol.* **199**, 783-798.

Duchen, M. R. (2000). Mitochondria and calcium: from cell signalling to cell death. *J. Physiol.* **529**, 57-68.

Giacomello, M., Drago, I., Bortolozzi, M., Scorzeto, M., Gianelle, A., Pizzo, P. and Pozzan, T. (2010). Ca2+ hot spots on the mitochondrial surface are generated by Ca2+ mobilization from stores, but not by activation of store-operated Ca2+ channels. *Mol. Cell* **38**, 280-290.

Giorgi, C., Ito, K., Lin, H. K., Santangelo, C., Wieckowski, M. R., Lebiedzinska, M., Bononi, A., Bonora, M., Duszynski, J., Bernardi, R. et al. (2010). PML regulates apoptosis at endoplasmic reticulum by modulating calcium release. *Science* **330**, 1247-1251.

Grynkiewicz, G., Poenie, M. and Tsien, R. Y. (1985). A new generation of Ca2+ indicators with greatly improved fluorescence properties. *J. Biol. Chem.* **260**, 3440-3450.

Hagar, R. E., Burgstahler, A. D., Nathanson, M. H. and Ehrlich, B. E. (1998). Type III InsP3 receptor channel stays open in the presence of increased calcium. *Nature* **396**, 81-84.

Hajnóczky, G. and Csordás, G. (2010). Calcium signalling: fishing out molecules of mitochondrial calcium transport. *Curr. Biol.* **20**, R888-R891.

Hanahan, D. and Weinberg, R. A. (2000). The hallmarks of cancer. *Cell* **100**, 57-70.

Hanahan, D. and Weinberg, R. A. (2011). Hallmarks of cancer: the next generation. *Cell* **144**, 646-674.

Hanson, C. J., Bootman, M. D., Distelhorst, C. W., Maraldi, T. and Roderick, H. L. (2008a). The cellular concentration of Bcl-2 determines its pro- or anti-apoptotic effect. *Cell Calcium* **44**, 243-258.

Hanson, C. J., Bootman, M. D., Distelhorst, C. W., Wojcikiewicz, R. J. and Roderick, H. L. (2008b). Bcl-2 suppresses Ca(2+) release through inositol 1,4,5-trisphosphate receptors and inhibits Ca(2+) uptake by mitochondria without affecting ER calcium store content. *Cell Calcium* **44**, 324-338.

Harzheim, D., Movassagh, M., Foo, R. S.-Y., Ritter, O., Tashfeen, A., Conway, S. J., Bootman, M. D. and Roderick, H. L. (2009). Increased InsP3Rs in the junctional sarcoplasmic reticulum augment Ca2+ transients and arrhythmias associated with cardiac hypertrophy. *Proc. Natl. Acad. Sci. USA* **106**, 11406-11411.

Hashii, M., Nozawa, Y. and Higashida, H. (1993). Bradykinin-induced cytosolic Ca2+ oscillations and inositol tetrakisphosphate-induced Ca2+ influx in voltage-clamped ras-transformed NIH/3T3 fibroblasts. *J. Biol. Chem.* **268**, 19403-19410.

Hattori, M., Suzuki, A. Z., Higo, T., Miyauchi, H., Michikawa, T., Nakamura, T., Inoue, T. and Mikoshiba, K. (2004). Distinct roles of inositol 1,4,5-trisphosphate receptor types 1 and 3 in Ca2+ signaling. *J. Biol. Chem.* **279**, 11967-11975.

Heighway, J., Betticher, D. C., Hoban, P. R., Altermatt, H. J. and Cowen, R. (1996). Coamplification in tumors of KRAS2, type 2 inositol 1,4,5 triphosphate receptor gene, and a novel human gene, KRAG. *Genomics* **35**, 207-214.

Higazi, D. R., Fearnley, C. J., Drawnel, F. M., Talasila, A., Corps, E. M., Ritter, O., McDonald, F., Mikoshiba, K., Bootman, M. D. and Roderick, H. L. (2009). Endothelin-1-stimulated InsP3-induced Ca2+ release is a nexus for hypertrophic signaling in cardiac myocytes. *Mol. Cell* **33**, 472-482.

Hovnanian, A. (2007). SERCA pumps and human diseases. *Subcell. Biochem.* **45**, 337-363.

Humez, S., Legrand, G., Vanden-Abeele, F., Monet, M., Marchetti, P., Lepage, G., Crepin, A., Dewailly, E., Wuytack, F. and Prevarskaya, N. (2004). Role of endoplasmic reticulum calcium content in prostate cancer cell growth regulation by IGF and TNFalpha. J. Cell. Physiol. 201, 201-213.

Kahl, C. R. and Means, A. R. (2003). Regulation of cell cycle progression by calcium/calmodulin-dependent pathways. Endocr. Rev. 24, 719-736.

Kasri, N. N., Holmes, A. M., Bultynck, G., Parys, J. B., Bootman, M. D., Rietdorf, K., Missiaen, L., McDonald, F., De Smedt, H., Conway, S. J. et al. (2004). Regulation of InsP3 receptor activity by neuronal Ca2+-binding proteins. EMBO J. 23, 312-321.

Kasri, N. N., Kocks, S. L., Verbert, L., Hébert, S. S., Callewaert, G., Parys, J. B., Missiaen, L. and De Smedt, H. (2006). Up-regulation of inositol 1,4,5-trisphosphate receptor type 1 is responsible for a decreased endoplasmic-reticulum Ca2+ content in presenilin double knock-out cells. Cell Calcium 40, 41-51.

Kelley, G. G., Reks, S. E., Ondrako, J. M. and Smrcka, A. V. (2001). Phospholipase C(epsilon): a novel ras effector. EMBO J. 20, 743-754.

Khan, A. A., Soloski, M. J., Sharp, A. H., Schilling, G., Sabatini, D. M., Li, S. H., Ross, C. A. and Snyder, S. H. (1996). Lymphocyte apoptosis: mediation by increased type 3 inositol 1,4,5-trisphosphate receptor. Science 273, 503-507.

Khan, M. T., Wagner, L., I, I, Yule, D. I., Bhanumathy, C. and Joseph, S. K. (2006). Akt kinase phosphorylation of inositol 1,4,5-trisphosphate receptors. J. Biol. Chem. 281, 3731-3737.

Kittler, R., Putz, G., Pelletier, L., Poser, I., Heninger, A. K., Drechsel, D., Fischer, S., Konstantinova, I., Habermann, B., Grabner, H. et al. (2004). An endoribonuclease-prepared siRNA screen in human cells identifies genes essential for cell division. Nature 432, 1036-1040.

Korošec, B., Glavac, D., Rott, T. and Ravnik-Glavac, M. (2006). Alterations in the ATP2A2 gene in correlation with colon and lung cancer. Cancer Genet. Cytogenet. 171, 105-111.

Lang, F., Friedrich, F., Kahn, E., Wöll, E., Hammerer, M., Waldegger, S., Maly, K. and Grunicke, H. (1991). Bradykinin-induced oscillations of cell membrane potential in cells expressing the Ha-ras oncogene. J. Biol. Chem. 266, 4938-4942.

Legrand, G., Humez, S., Slomianny, C., Dewailly, E., Vanden Abeele, F., Mariot, P., Wuytack, F. and Prevarskaya, N. (2001). Ca2+ pools and cell growth. Evidence for sarcoendoplasmic Ca2+-ATPases 2B involvement in human prostate cancer cell growth control. J. Biol. Chem. 276, 47608-47614.

Lipskaia, L., Hulot, J. S. and Lompré, A. M. (2009). Role of sarco/endoplasmic reticulum calcium content and calcium ATPase activity in the control of cell growth and proliferation. Pflugers Arch. 457, 673-685.

Little, A. S., Smith, P. D. and Cook, S. J. (2013). Mechanisms of acquired resistance to ERK1/2 pathway inhibitors. Oncogene 32, 1207-1215.

Marchi, S., Marinello, M., Bononi, A., Bonora, M., Giorgi, C., Rimessi, A. and Pinton, P. (2012). Selective modulation of subtype III IP$_3$R by Akt regulates ER Ca^{2+} release and apoptosis. Cell Death Dis. 3, e304.

Mendes, C. C., Gomes, D. A., Thompson, M., Souto, N. C., Goes, T. S., Goes, A. M., Rodrigues, M. A., Gomez, M. V., Nathanson, M. H. and Leite, M. F. (2005). The type III inositol 1,4,5-trisphosphate receptor preferentially transmits apoptotic Ca2+ signals into mitochondria. J. Biol. Chem. 280, 40892-40900.

Miyakawa, T., Maeda, A., Yamazawa, T., Hirose, K., Kurosaki, T. and Iino, M. (1999). Encoding of Ca2+ signals by differential expression of IP3 receptor subtypes. EMBO J. 18, 1303-1308.

Monteith, G. R., McAndrew, D., Faddy, H. M. and Roberts-Thomson, S. J. (2007). Calcium and cancer: targeting Ca2+ transport. Nat. Rev. Cancer 7, 519-530.

Monteith, G. R., Davis, F. M. and Roberts-Thomson, S. J. (2012). Calcium channels and pumps in cancer: changes and consequences. J. Biol. Chem. 287, 31666-31673.

Motiani, R. K., Hyzinski-García, M. C., Zhang, X., Henkel, M. M., Abdullaev, I. F., Kuo, Y. H., Matrougui, K., Mongin, A. A. and Trebak, M. (2013). STIM1 and Orai1 mediate CRAC channel activity and are essential for human glioblastoma invasion. Pflugers Arch. 465, 1249-1260.

Oakes, S. A., Scorrano, L., Opferman, J. T., Bassik, M. C., Nishino, M., Pozzan, T. and Korsmeyer, S. J. (2005). Proapoptotic BAX and BAK regulate the type 1 inositol trisphosphate receptor and calcium leak from the endoplasmic reticulum. Proc. Natl. Acad. Sci. USA 102, 105-110.

Orrenius, S., Zhivotovsky, B. and Nicotera, P. (2003). Regulation of cell death: the calcium-apoptosis link. Nat. Rev. Mol. Cell Biol. 4, 552-565.

Palmer, A. E., Jin, C., Reed, J. C. and Tsien, R. Y. (2004). Bcl-2-mediated alterations in endoplasmic reticulum Ca2+ analyzed with an improved genetically encoded fluorescent sensor. Proc. Natl. Acad. Sci. USA 101, 17404-17409.

Peppiatt, C. M., Collins, T. J., Mackenzie, L., Conway, S. J., Holmes, A. B., Bootman, M. D., Berridge, M. J., Seo, J. T. and Roderick, H. L. (2003). 2-Aminoethoxydiphenyl borate (2-APB) antagonises inositol 1,4,5-trisphosphate-induced calcium release, inhibits calcium pumps and has a use-dependent and slowly reversible action on store-operated calcium entry channels. Cell Calcium 34, 97-108.

Pinton, P., Ferrari, D., Rapizzi, E., Di Virgilio, F., Pozzan, T. and Rizzuto, R. (2001). The Ca2+ concentration of the endoplasmic reticulum is a key determinant of ceramide-induced apoptosis: significance for the molecular mechanism of Bcl-2 action. EMBO J. 20, 2690-2701.

Pinton, P., Giorgi, C., Siviero, R., Zecchini, E. and Rizzuto, R. (2008). Calcium and apoptosis: ER-mitochondria Ca2+ transfer in the control of apoptosis. Oncogene 27, 6407-6418.

Prasad, V., Boivin, G. P., Miller, M. L., Liu, L. H., Erwin, C. R., Warner, B. W. and Shull, G. E. (2005). Haploinsufficiency of Atp2a2, encoding the sarco(endo)plasmic reticulum Ca2+-ATPase isoform 2 Ca2+ pump, predisposes mice to squamous cell tumors via a novel mode of cancer susceptibility. Cancer Res. 65, 8655-8661.

Rizzuto, R. and Pozzan, T. (2006). Microdomains of intracellular Ca2+: molecular determinants and functional consequences. Physiol. Rev. 86, 369-408.

Rizzuto, R., Pinton, P., Carrington, W., Fay, F. S., Fogarty, K. E., Lifshitz, L. M., Tuft, R. A. and Pozzan, T. (1998). Close contacts with the endoplasmic reticulum as determinants of mitochondrial Ca2+ responses. Science 280, 1763-1766.

Rizzuto, R., Pinton, P., Ferrari, D., Chami, M., Szabadkai, G., Magalhães, P. J., Di Virgilio, F. and Pozzan, T. (2003). Calcium and apoptosis: facts and hypotheses. Oncogene 22, 8619-8627.

Rizzuto, R., Duchen, M. R. and Pozzan, T. (2004). Flirting in little space: the ER/mitochondria Ca2+ liaison. Sci. STKE 2004, re1.

Rizzuto, R., De Stefani, D., Raffaello, A. and Mammucari, C. (2012). Mitochondria as sensors and regulators of calcium signalling. Nat. Rev. Mol. Cell Biol. 13, 566-578.

Roderick, H. L. and Cook, S. J. (2008). Ca2+ signalling checkpoints in cancer: remodelling Ca2+ for cancer cell proliferation and survival. Nat. Rev. Cancer 8, 361-375.

Roderick, H. L., Campbell, A. K. and Llewellyn, D. H. (1997). Nuclear localisation of calreticulin in vivo is enhanced by its interaction with glucocorticoid receptors. FEBS Lett. 405, 181-185.

Sakakura, C., Hagiwara, A., Fukuda, K., Shimomura, K., Takagi, T., Kin, S., Nakase, Y., Fujiyama, J., Mikoshiba, K., Okazaki, Y. et al. (2003). Possible involvement of inositol 1,4,5-trisphosphate receptor type 3 (IP3R3) in the peritoneal dissemination of gastric cancers. Anticancer Res. 23 5A, 3691-3697.

Schulze, A., Nicke, B., Warne, P. H., Tomlinson, S. and Downward, J. (2004). The transcriptional response to Raf activation is almost completely dependent on mitogen-activated protein kinase kinase activity and shows a major autocrine component. Mol. Biol. Cell 15, 3450-3463.

Serrano, M., Lin, A. W., McCurrach, M. E., Beach, D. and Lowe, S. W. (1997). Oncogenic ras provokes premature cell senescence associated with accumulation of p53 and p16INK4a. Cell 88, 593-602.

Shirasawa, S., Furuse, M., Yokoyama, N. and Sasazuki, T. (1993). Altered growth of human colon cancer cell lines disrupted at activated Ki-ras. Science 260, 85-88.

Szabadkai, G. and Duchen, M. R. (2008). Mitochondria: the hub of cellular Ca2+ signaling. Physiology (Bethesda) 23, 84-94.

Szado, T., Vanderheyden, V., Parys, J. B., De Smedt, H., Rietdorf, K., Kotelevets, L., Chastre, E., Khan, F., Landegren, U., Söderberg, O. et al. (2008). Phosphorylation of inositol 1,4,5-trisphosphate receptors by protein kinase B/Akt inhibits Ca2+ release and apoptosis. Proc. Natl. Acad. Sci. USA 105, 2427-2432.

Szatkowski, C., Parys, J. B., Ouadid-Ahidouch, H. and Matifat, F. (2010). Inositol 1,4,5-trisphosphate-induced Ca2+ signalling is involved in estradiol-induced breast cancer epithelial cell growth. Mol. Cancer 9, 156.

Thomas, D., Lipp, P., Tovey, S. C., Berridge, M. J., Li, W., Tsien, R. Y. and Bootman, M. D. (2000). Microscopic properties of elementary Ca2+ release sites in non-excitable cells. Curr. Biol. 10, 8-15.

Tuveson, D. A., Shaw, A. T., Willis, N. A., Silver, D. P., Jackson, E. L., Chang, S., Mercer, K. L., Grochow, R., Hock, H., Crowley, D. et al. (2004). Endogenous oncogenic K-ras(G12D) stimulates proliferation and widespread neoplastic and developmental defects. Cancer Cell 5, 375-387.

Vartanian, S., Bentley, C., Brauer, M. J., Li, L., Shirasawa, S., Sasazuki, T., Kim, J. S., Haverty, P., Stawiski, E., Modrusan, Z. et al. (2013). Identification of mutant K-Ras-dependent phenotypes using a panel of isogenic cell lines. J. Biol. Chem. 288, 2403-2413.

Wakelam, M. J., Davies, S. A., Houslay, M. D., McKay, I., Marshall, C. J. and Hall, A. (1986). Normal p21N-ras couples bombesin and other growth factor receptors to inositol phosphate production. Nature 323, 173-176.

Weber, G. (2005). Down-regulation of increased signal transduction capacity in human cancer cells. Adv. Enzyme Regul. 45, 37-51.

Wu, W. K., Wang, X. J., Cheng, A. S., Luo, M. X., Ng, S. S., To, K. F., Chan, F. K., Cho, C. H., Sung, J. J. and Yu, J. (2013). Dysregulation and crosstalk of cellular signaling pathways in colon carcinogenesis. Crit. Rev. Oncol. Hematol. 86, 251-277.

Wuytack, F., Eggermont, J. A., Raeymaekers, L., Plessers, L. and Casteels, R. (1989). Antibodies against the non-muscle isoform of the endoplasmic reticulum Ca2(+)-transport ATPase. Biochem. J. 264, 765-769.

Wuytack, F., Papp, B., Verboomen, H., Raeymaekers, L., Dode, L., Bobe, R., Enouf, J., Bokkala, S., Authi, K. S. and Casteels, R. (1994). A sarco/endoplasmic reticulum Ca(2+)-ATPase 3-type Ca2+ pump is expressed in platelets, in lymphoid cells, and in mast cells. J. Biol. Chem. 269, 1410-1416.

Yoshida, J., Iwabuchi, K., Matsui, T., Ishibashi, T., Masuoka, T. and Nishio, M. (2012). Knockdown of stromal interaction molecule 1 (STIM1) suppresses store-operated calcium entry, cell proliferation and tumorigenicity in human epidermoid carcinoma A431 cells. Biochem. Pharmacol. 84, 1592-1603.
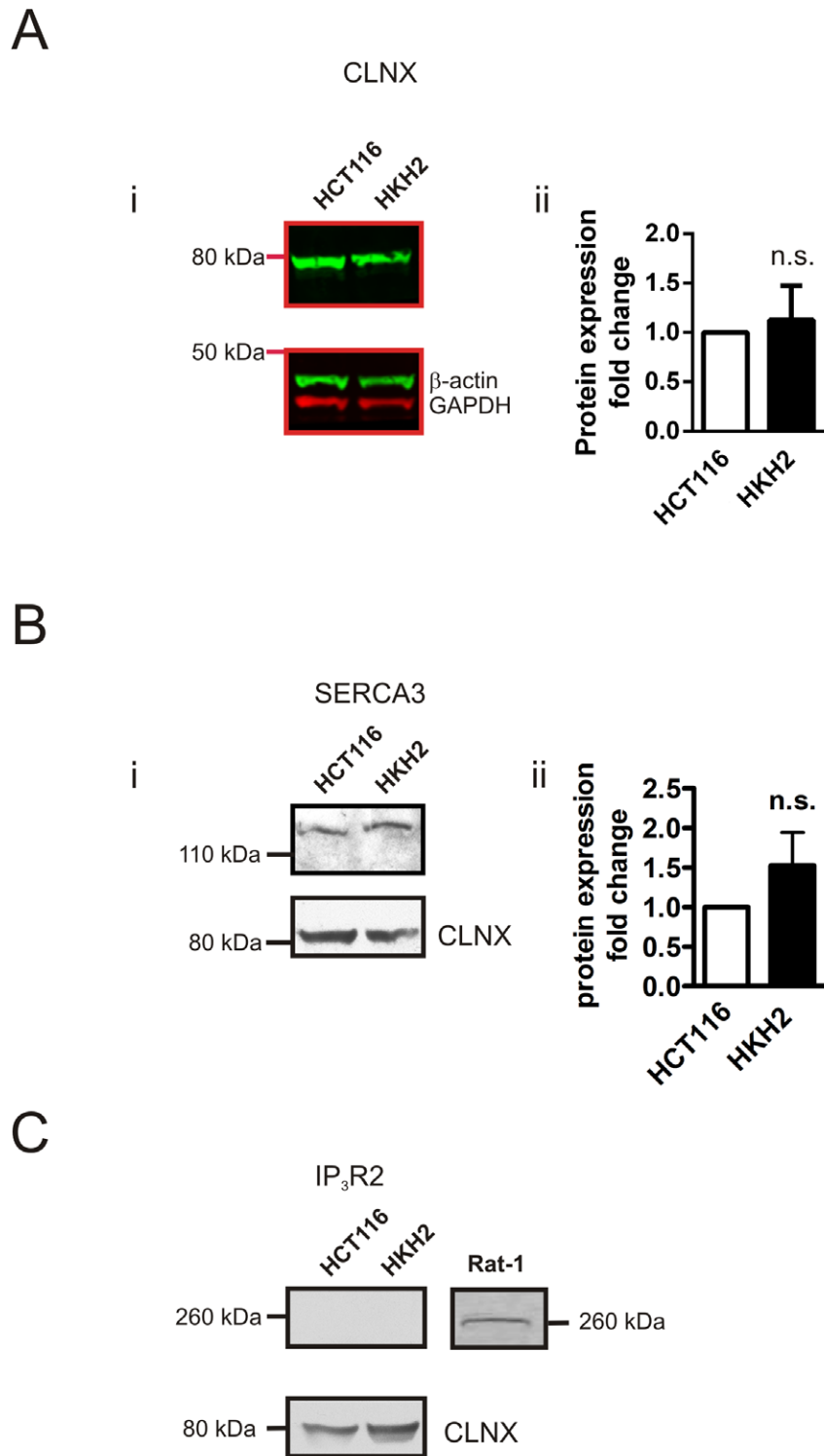
Fig. S1. (**A**) Expression of calnexin in lysates prepared from HCT116 and HKH2 cells. (**i**) Representative immunoblot of calnexin. GAPDH and beta-actin are used as a loading control. (**ii**) Fold change in calnexin expression in HKH2 cells with respect to HCT116 cells. Bar graph represents the mean ± SEM (n=6). Expression of calnexin was not significantly different between HCT116 and HKH2 (one-sample *t*-test).

(**B**) Expression of SERCA3 in lysates prepared from HCT116 and HKH2 cells. (**i**) Representative immunoblot of SERCA3. Calnexin is used as a loading control. (**ii**) Fold change in SERCA3 expression in HKH2 cells with respect to HCT116 cells. Bar graph represents the mean ± SEM (n=8). Expression of SERCA3 was not significantly different between HCT116 and HKH2 (one-sample *t*-test).

(**C**) Expression of IP$_3$R2 in lysates prepared from HCT116 and HKH2 cells. Representative immunoblot of IP$_3$R2 in HCT116, HKH2 and Rat1 fibroblasts. Calnexin is used as a loading control. An equivalent amount of protein lysate to that used for detection of IP$_3$Rs in HCT116 and HKH2 cells prepared from the Rat-1 fibroblast cell line was used as a positive control for detection of IP$_3$R2.
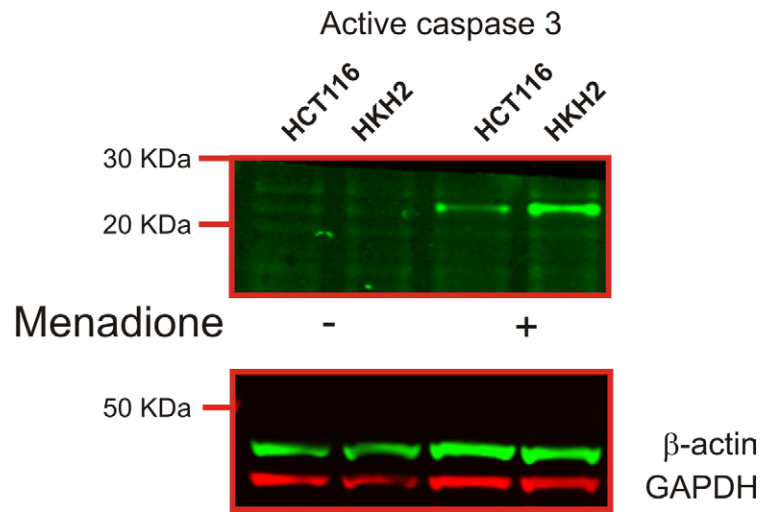
Fig. S2. Immunoblot of activated caspase 3 in HCT and HKH2 cells exposed to menadione for 20 h. Lysates prepared from naïve and menadione exposed HCT116 and HKH2 cells were resolved by SDS PAGE and transferred to nitrocellulose. Blots were probed with antibodies directed against activated (cleaved) caspase and against β-actin and GAPDH, which were used as controls for equivalent loading. Fluorescently labeled secondary antibodies were detected using the LI-COR Odyssey imaging system.